Report No. M-32

PRELIMINARY RADAR SYSTEMS ANALYSIS FOR VENUS ORBITER MISSIONS

Report No. M-32

PRELIMINARY RADAR SYSTEMS ANALYSIS FOR VENUS ORBITER MISSIONS

by

R. K. Brandenburg

and

D. J. Spadoni

Astro Sciences

of

IIT Research Institute
Chicago, Illinois

for

Planetary Programs Division

Office of Space Science and Application
NASA Headquarters
Washington, D. C.

Contract No. NASW-2144

Approved by:

D L Roberts

D. L. Roberts, Manager
Astro Sciences

November, 1971

PRELIMINARY RADAR SYSTEMS ANALYSIS FOR VENUS ORBITER MISSIONS

SUMMARY

This report consists of a short, preliminary analysis of the problems involved in mapping the surface of Venus with radar from an orbiting spacecraft. Two types of radar, the non-coherent sidelooking and the focused synthetic aperture systems, are sized to fulfill two assumed "levels" of Venus exploration. Spacecraft are scaled to accommodate the radars' requirements, and the applicability of ballistic and solar electric delivery modes for the types of missions this analysis suggests is examined.

The two "exploration levels", regional and local, assumed for this study are based on previous Astro Sciences work (Klopp 1969). The regional level is defined as 1 to 3 kilometer spatial and 0.5 to 1 km vertical resolution of 100 percent of the planet's surface. The local level is defined as 100 to 200 meter spatial and 50-100 m vertical resolution of about 10 percent of the surface (based on the regional survey).

Earth-based radar studies of Venus have found that the radar cross section rapidly decreases for wavelengths shorter than 10 cm. The size of the spacecraft's radar antenna is directly proportional to the operating wavelength and thus to keep the antenna's dimensions small it is necessary to choose as short a wavelength as possible. Therefore for this study a 10 cm operating frequency was chosen for both radar systems in order to minimize the antenna size and maximize the apparent radar cross section of the surface.

An initial exploratory analysis was performed to determine the approximate resolution region of interest for each radar system. From this investigation it was determined that noncoherent radar appears to be best suited for regional coverage and synthetic aperture for local coverage. A more detailed analysis was then performed and each radar system sized to perform at its respective coverage level at altitudes between 300 and 1300 km (polar circular orbits). The antenna sizes for the two radars are shown in Summary Figure 1. The noncoherent system's antenna was sized to provide an azimuthal resolution of 3 km up to an altitude of 700 km where the antenna length was fixed at 50 m. At altitudes above 700 km, the ground resolution degrades, reaching 6 km at 1300 km altitude.

The synthetic aperture antenna was sized to provide ground resolutions of 100 and 200 m. The synthetic aperture antenna length is less constrained by altitude and beamwidth than the noncoherent system, and the length actually decreases with increasingly finer resolution. The decrease in antenna size is balanced by the increase in input power for finer resolution with the synthetic aperture system. Summary Figure 2 illustrates the variation in required input power with altitude for the two radars. The noncoherent system requires relatively low powers, about 100 watts, for kilometer scale resolution, while the synthetic aperture system may require up to 26 kilowatts for 100 m resolution from high altitudes.

Summary Figure 3 shows the variation in total system weight (antenna plus electronics) for the two types of radar. The noncoherent system is dominated by the antenna weight, as is illustrated by the sharp bend in the curve at the point where the antenna is fixed at 1.5 x 50 m. There are two effects showing up in the synthetic aperture system weights. The 100 m resolution system requires a smaller (and lighter weight) antenna than the 200 m system, but also requires heavier electronics due to higher peak powers. The two effects offset each other to yield a slower weight growth rate with altitude.

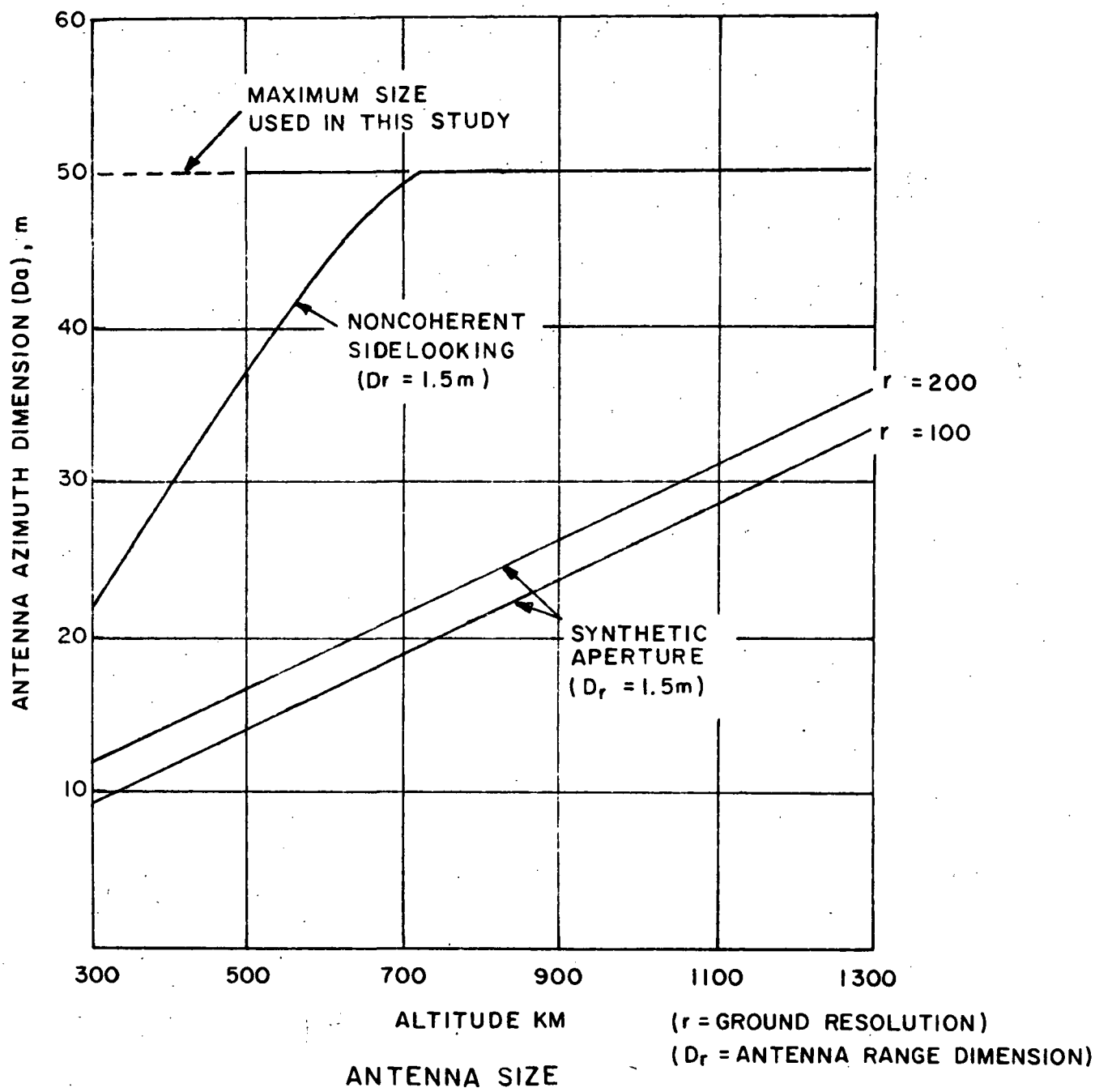

ANTENNA SIZE

SUMMARY FIGURE I.

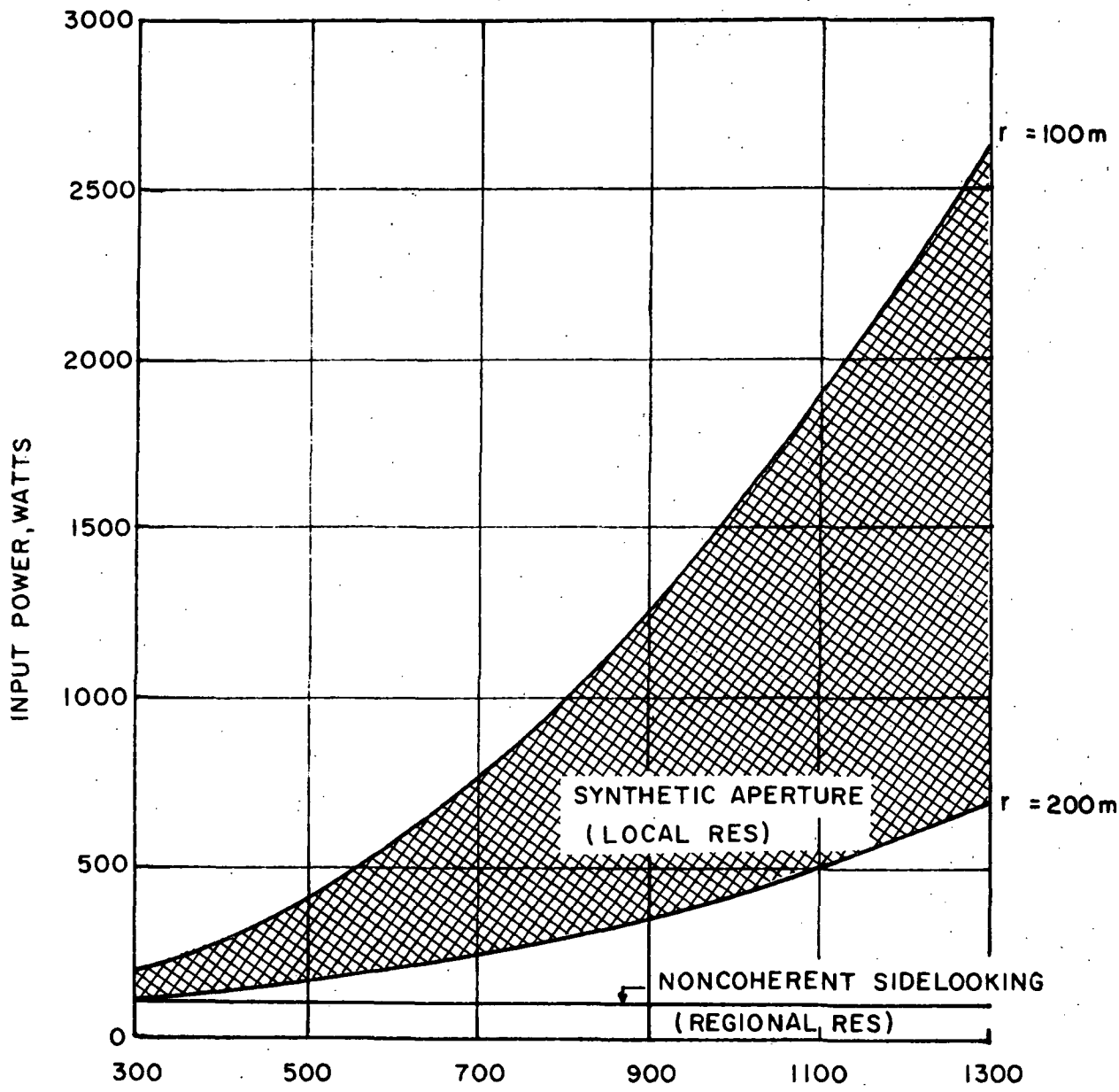

INPUT POWER

SUMMARY FIGURE 2.

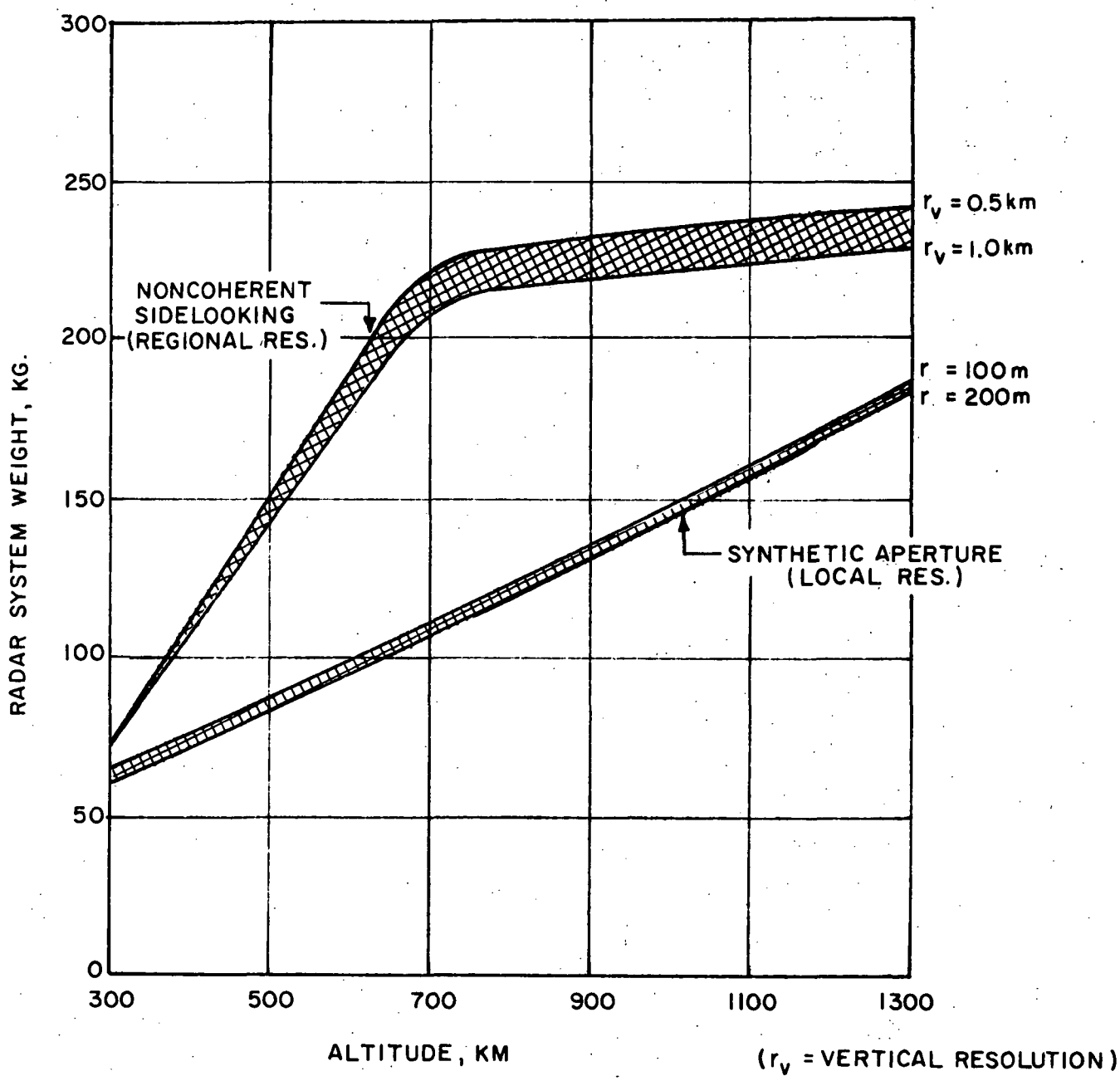

TOTAL RADAR SYSTEM WEIGHT
(ANTENNA & ELECTRONICS)

SUMMARY FIGURE 3.

Due to the low, circular orbits chosen for this study the radar mapping spacecraft will be occulted from the sun and earth for as much as 0.6 hours per orbit. If the spacecraft is powered by solar panels only, it will be able to map 75 percent of the planet's surface during a nominal 120 day mission (worst case conditions). If, however, it uses a sun-independent power system, such as RTG's or solar panels and batteries, it will not be affected by solar occultation and can map 100 percent of the surface in 120 days.

The data telemetry rate is also affected by these occultations. Data is acquired at rates up to 4400 bps for the noncoherent system and up to 2.5×10^6 bps for the synthetic aperture system. However, due to the small swath widths chosen (50-250 km) and the slow sidereal rotation of Venus (1.5°/24 hours), the spacecraft must wait between 4 and 18 orbits after mapping a swath until the next swath comes into view. Using this time to transmit acquired data the bit rates can be reduced to about 1000 bps for noncoherent and 2.5×10^5 bps for synthetic aperture. A review of the key radar parameters for both the noncoherent sidelooking and synthetic aperture systems is provided in Summary Table 1.

Summary Figure 4 illustrates the variation in spacecraft weight, sized to accommodate the radar systems. RTGs were used as the power supply up to the point where the radar required more than 750 watts of input power. At this point the solar panels of an SEP stage were used as the power supply (the SEP stage weights are not included on this figure, but are taken into account for the payload analysis). An RTG powered system was preferred because the spacecraft pointing problems, already significant due to the long antennas, are only complicated by the use of solar panels for power. However, a combined solar panel/battery power system (also shown in Summary Figure 4) which utilizes stored battery power when mapping thereby eliminating control conflicts between the panels and radar antenna, was found to be an attractive

SUMMARY TABLE 1

VENUS ORBITER RADAR SYSTEM CHARACTERISTICS

SYSTEM CHARACTERISTICS	RADAR	
	NONCOHERENT SIDELOOKING	SYNTHETIC APERTURE
Resolution	0.5 x 3 km	100 x 100 m
Antenna	1.5 x 50 m (at 700 km alt.)	1.5 x 20 m (at 700 km alt.)
Radar Input Power	~ 100 watts	0.1 - 2.6 kw
System Weight	~ 75-240 kg	~ 60-180 kg
Data Rate (Telemetry)	~ 10^3 bps	~ 10^4 - 10^5 bps
Data Storage	~ 2 x 10^8 bits	~ 4 x 10^9 bits

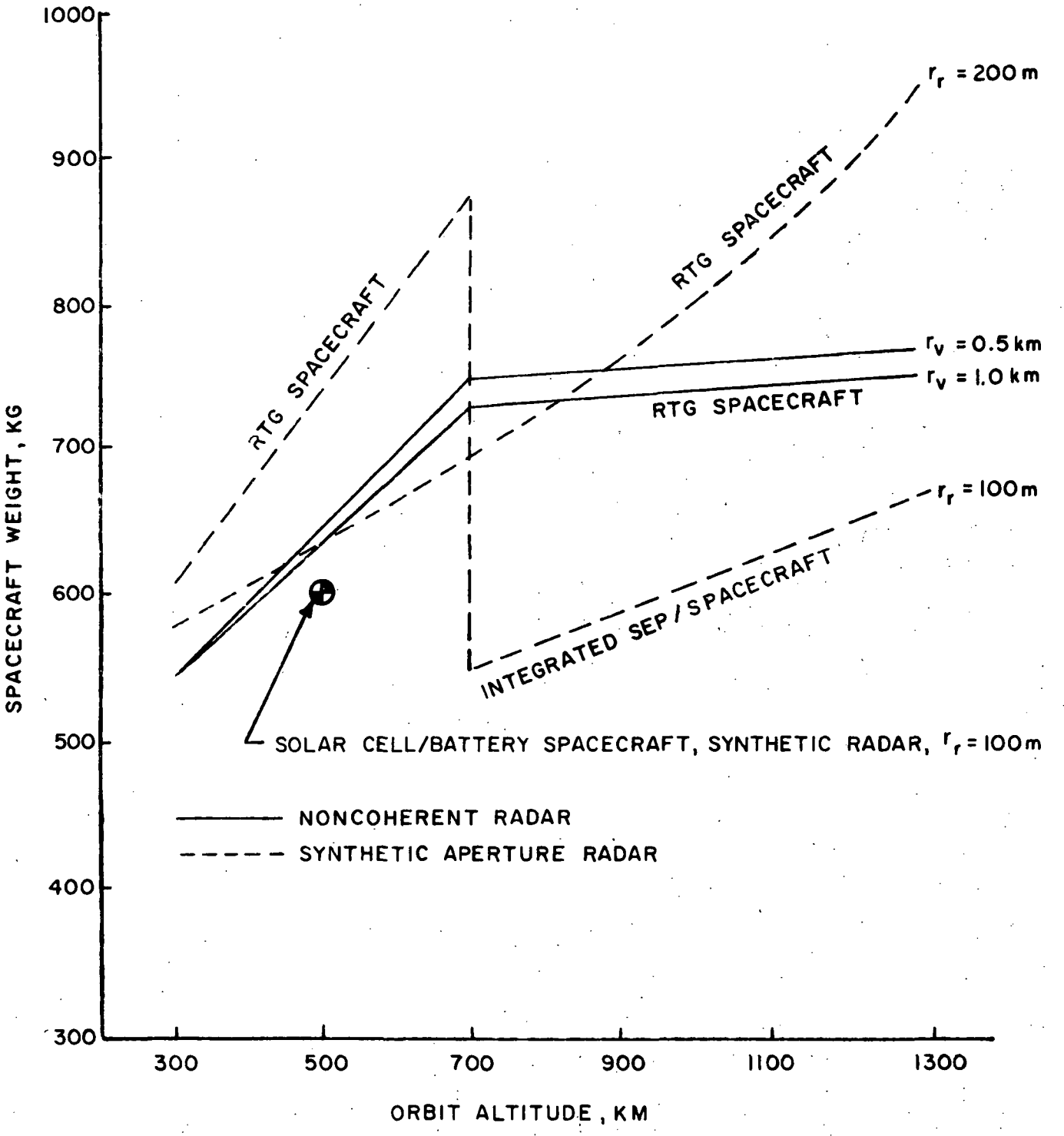

VENUS RADAR MAPPING SPACECRAFT, REQUIRED WEIGHT IN ORBIT.

SUMMARY FIGURE 4.

alternative to an RTG power source. The spacecraft communications and data storage systems were based on Mariner '73 and TOPS technology.

The payload capability (net spacecraft weight in orbit) of the Titan IIID/Centaur was analyzed for five launch dates. Of these the '83 and '84 launch dates provided enough payload for practically all missions, including the lower altitude ones (which are preferable because of smaller antenna sizes). The '81 launch is adequate for a few low altitude missions, but the '78 and '80 opportunities are completely inadequate for these missions. Two dimensional solar electric propulsion data was also analyzed and the Titan IIID/Centaur with a 3.7 kilowatt SEP stage was found to provide ample payload in orbit for all missions.

This study has demonstrated the feasibility of mapping Venus from a radar orbiter. The noncoherent system can provide resolutions of several kilometers but with practical limits on antenna size cannot map at lower resolutions. The focused synthetic aperture radar, however, is not constrained by antenna size and has a very large growth potential. It is clear from this study that 100 percent of the planet's surface can be mapped at 100 m-200 m using synthetic aperture radar for about the same cost in weight as a 3-km resolution, noncoherent radar.

The trade-offs between solar panels and RTG's still need further study. The RTG system does not have the pointing problems that solar panels do, but this advantage for radar mapping, may be outweighed by the thermal problems resulting in the use of multiple RTG power units. Also the communications and data handling systems necessary for synthetic aperture radar require further study. The requirements identified in this study are certainly not impossible but do approach current technological limits.

PRELIMINARY RADAR SYSTEMS ANALYSIS

FOR VENUS ORBITER MISSIONS

TABLE OF CONTENTS

TABLE OF CONTENTS (continued)

LIST OF FIGURES

LIST OF FIGURES (continued)

LIST OF TABLES

PRELIMINARY RADAR SYSTEMS ANALYSIS FOR VENUS ORBITER MISSIONS

1. INTRODUCTION

It is generally agreed by most scientists and mission planners that the only way to obtain a surface map of Venus is through the use of radar, due to the apparently impenetrable cloud cover. Earth-based radar is constrained, by the large distance involved and Venus' earth-synchronous rotation, to view only a fraction of the Venusian surface at very poor resolutions. Using advanced techniques a region approximately 80° in latitude by 100° in longitude on the earth-facing (inferior conjunction) surface has been mapped at resolutions down to about 40 km. Figure 1 presents a radar map of Venus with a best ground resolution of about 100 km obtained with the MIT Haystack-Westford interferometer (Rogers and Ingalls 1969). In the future system improvements will produce best resolutions down to perhaps 4 km over a small fraction of the planet's surface. It is certain however that in the foreseeable future earth-based radar will never provide the resolutions and coverage consistent with the desires of planetary scientists. Orbiting, radar equipped spacecraft are an obvious solution to the problems involved in mapping Venus.

This study concerns itself with a preliminary evaluation of two types of radar systems, the Noncoherent Side-Looker and the Focused Synthetic Aperture, for use in mapping the Venusian surface. Although neither radar system has yet been developed for use in a spacecraft, both have been flown in aircraft mapping parts of the earth (the synthetic aperture being used for this just recently). Hopefully from this analysis the reader will be able to judge the relative merits of each type of radar. However, it must be kept in mind that this is a simplified preliminary analysis, and not an actual mission definition.

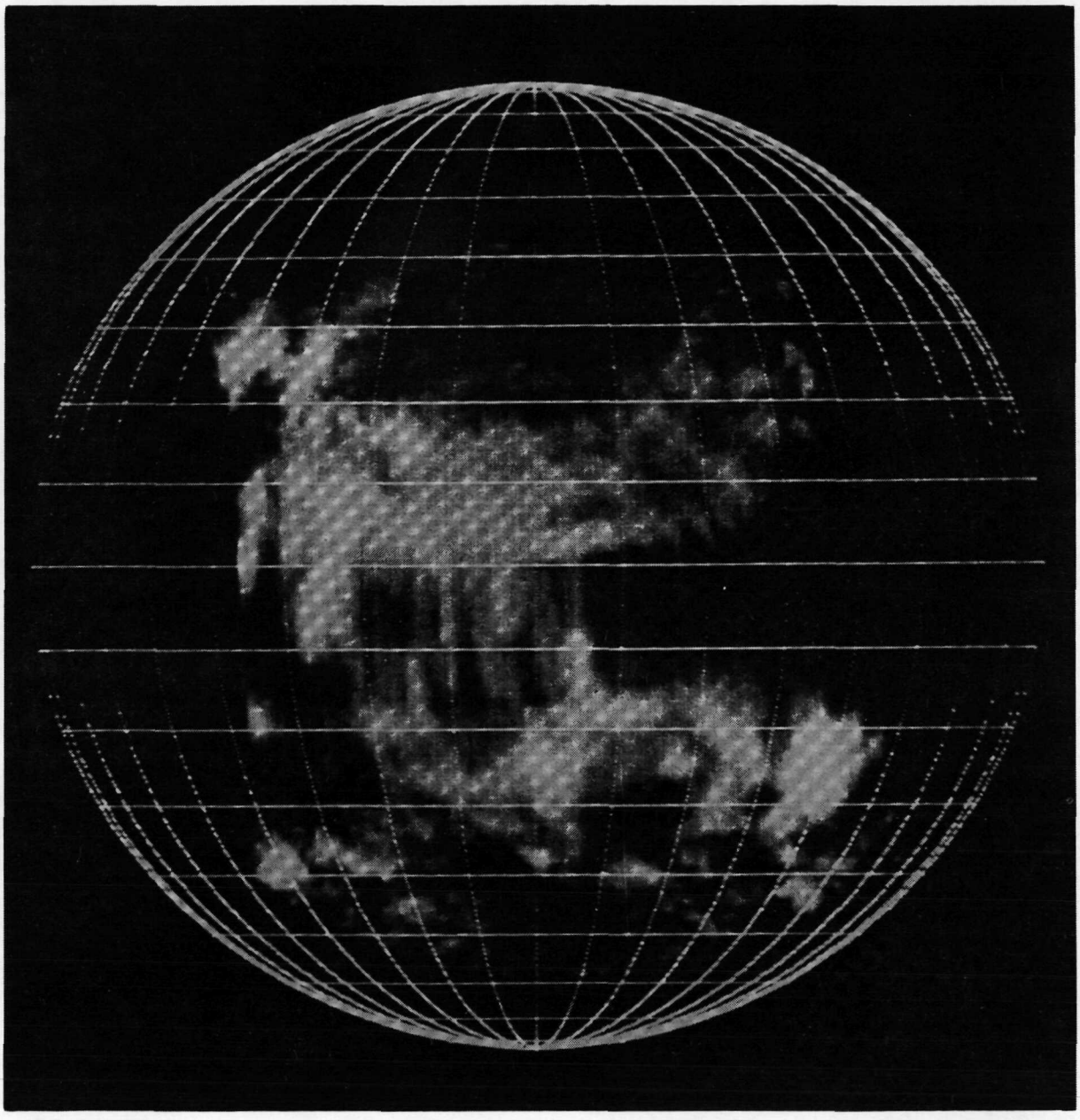

FIGURE 1.

RADAR BACKSCATTER INTENSITY MAP OF VENUS AT 3.8cm

(Rodgers and Ingalls 1970)

It was assumed for this study that the radar systems satisfy the requirements of one of two levels of exploration. The Regional level is defined as 1 to 3 kilometer spatial and 0.5 to 1 kilometer vertical resolution with 75 to 100 percent coverage of Venus' surface. The Local level is defined as 100 to 200 meter spatial and 50 to 100 meter vertical resolution with about 10 percent surface coverage. The local coverage is of those areas singled out by the regional mapping to be of special interest. These resolution levels are based on the findings of a previous Astro Sciences study (Klopp 1969) wherein the scientific objectives of Venus exploration were considered.

The ranges in resolution over which Noncoherent and Synthetic Aperture Radars are most efficient in terms of weight are discussed in Section 2. The methodology developed to semi-optimize the two radar system parameters is then set down and the variations in antenna dimensions, power, weight and data rate with changing measurement specifications are illustrated. In Section 3 these raw parameters are used to size the spacecraft requirements. With this data and the trajectory and payload analysis (also performed in Section 3) several launch vehicles and upper stages are evaluated. Representative or sample missions are then discussed in detail. Section 4 draws together the conclusions of this study and contains recommendations for further study.

2. THE RADAR MAPPING ORBITER

2.1 Basics of Noncoherent and Synthetic Aperture Radar Resolution

Noncoherent radar achieves two dimensional ground resolution through the use of two methods. In the direction of spacecraft motion (the azimuth direction) the ground resolution is essentially that length which is illuminated by the radar beam as illustrated by Figure 2. Azimuth resolution, r_a, is therefore proportional to the antenna beamwidth in that dimension. This beamwidth is inversely proportional to the antenna's azimuth dimension which means that the azimuth dimension must increase as the azimuth resolution improves.

Resolution perpendicular to the direction of motion is achieved using echo time delay. A pulse is generated by the radar system, bounced off the target area, and its echo analyzed by delay time. Referring to Figure 2, range resolution r_r, can be expressed as,

$$r_r \cong \frac{1}{2} \frac{c\,\tau}{\cos \Psi} \qquad (2.1)$$

where c is the velocity of the radar wave, τ is the pulse width (in seconds) and Ψ is the grazing angle. The range resolution is then directly proportional to the pulse width. Note that range resolution cannot be obtained directly under the spacecraft ($\Psi = 90°$).

The swath width on the planet's surface is that area which falls within the radar antenna's range beamwidth. The swath width is inversely proportional to the range dimension of the antenna.

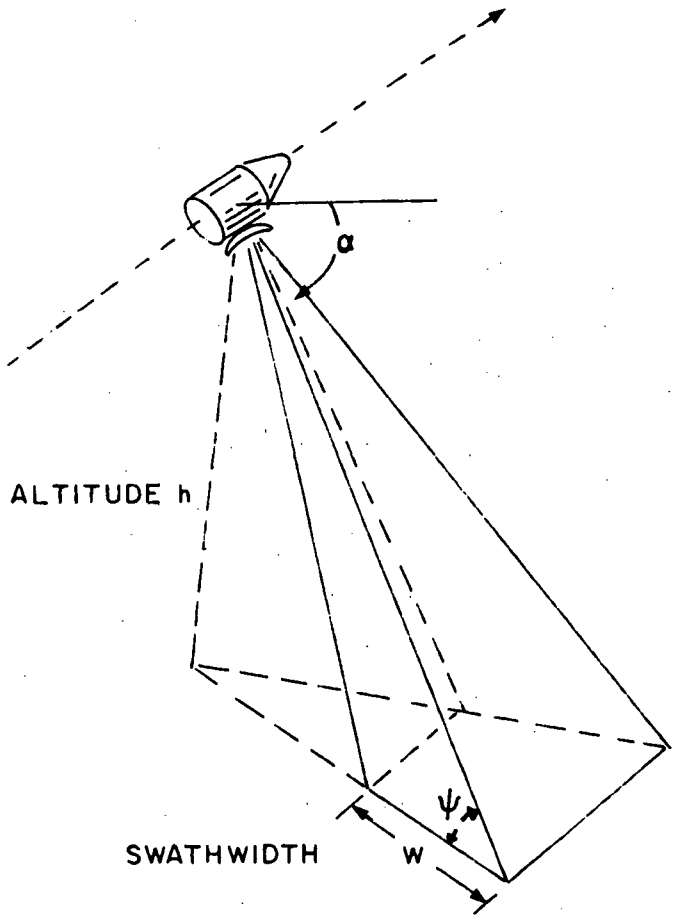

SYNTHETIC APERTURE RADAR
RESOLUTION ELEMENTS

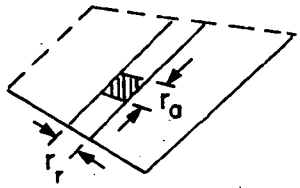

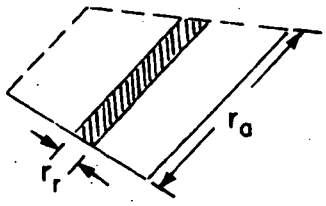

NONCOHERENT SIDELOOKING RADAR
RESOLUTION ELEMENTS

(r_r = RANGE RESOLUTION)
(r_a = AZIMUTH RESOLUTION)

FIGURE 2. SIDE-LOOKING RADAR GEOMETRY.

Vertical resolution can be obtained by the noncoherent radar through the shadowing of the range elements. Vertical resolution, r_v, is then,

$$r_v \cong r_r \tan \Psi \tag{2.2}$$

The ground resolution element for noncoherent radar, as shown in Figure 2, is constrained by the above relationships and practical antenna restrictions to be elongated in the azimuth direction. As will be shown later, the rectangular resolution element is the best that can be obtained with noncoherent radar.

Synthetic aperture radar overcomes the poor aximuth resolution of noncoherent radar by synthetically creating a long linear antenna. With each pulse transmission, as the real antenna moves over a fixed path, a new element of the synthetic antenna is generated. In the focused mode a phase shift is applied to the returning pulse to account for the spherical (rather than planar) wave. The resultant azimuth resolution is much smaller than the beamwidth of the physical antenna. This is approximately,

$$r_a \cong \frac{\lambda R_s}{2D_{sa}} \tag{2.3}$$

where λ is the wavelength, R_s the slant range, and D_{sa} the total length of the synthetic aperture. The length of the synthetic aperture is constrained by a number of factors as will be seen later.

The range resolution, vertical resolution, and swath width are all essentially the same for synthetic aperture as for noncoherent radar. However with synthetic aperture a square ground resolution element is possible to obtain, which is more easily interpreted than the elongated cell of noncoherent.

For both radar systems the resolution is also dependent on the depression angle, α (see Fig. 2). For the low altitude or "flat planet" case the range resolution for both systems degrades to 1/2 its maximum value when $\alpha > 60°$. For the synthetic aperture system aximuth resolution degrades to 1/2 its maximum value when $\alpha < 30°$ (Greenberg, 1967). Thus for this study the depression angle for both radars has been fixed at 45°.

2.2 Wavelength Selection

It is known from previous experience that spacecraft radar antennas necessary for regional-local resolution are generally quite large (Goldman and Brandenburg 1971). Fundamental antenna theory states that the dimension of an antenna is directly proportional to the wavelength ($D \propto \lambda$). Therefore in order to keep the antenna small it is best to pick an operating wavelength as short as possible, keeping in mind the radar cross section. Figure 3 shows the variation in Venus' normalized cross section with wavelength. The curve is fairly flat at wavelengths above 10 cm, but falls off rapidly at shorter wavelengths. Since models of the Venusian atmosphere predict only a small amount of atmospheric attenuation at a wavelength of 10 cm, it is advisable, then, to pick a wavelength in that spectral region. Thus for all the radar systems investigated in this study, a 10 cm operating wavelength was used.

2.3 Selection of Resolution Ranges for Noncoherent and Synthetic Aperture Radar Systems

Figure 4 illustrates the variation in system weight with resolution for the two radar systems of interest. The weights shown are based entirely on the radar electronics and

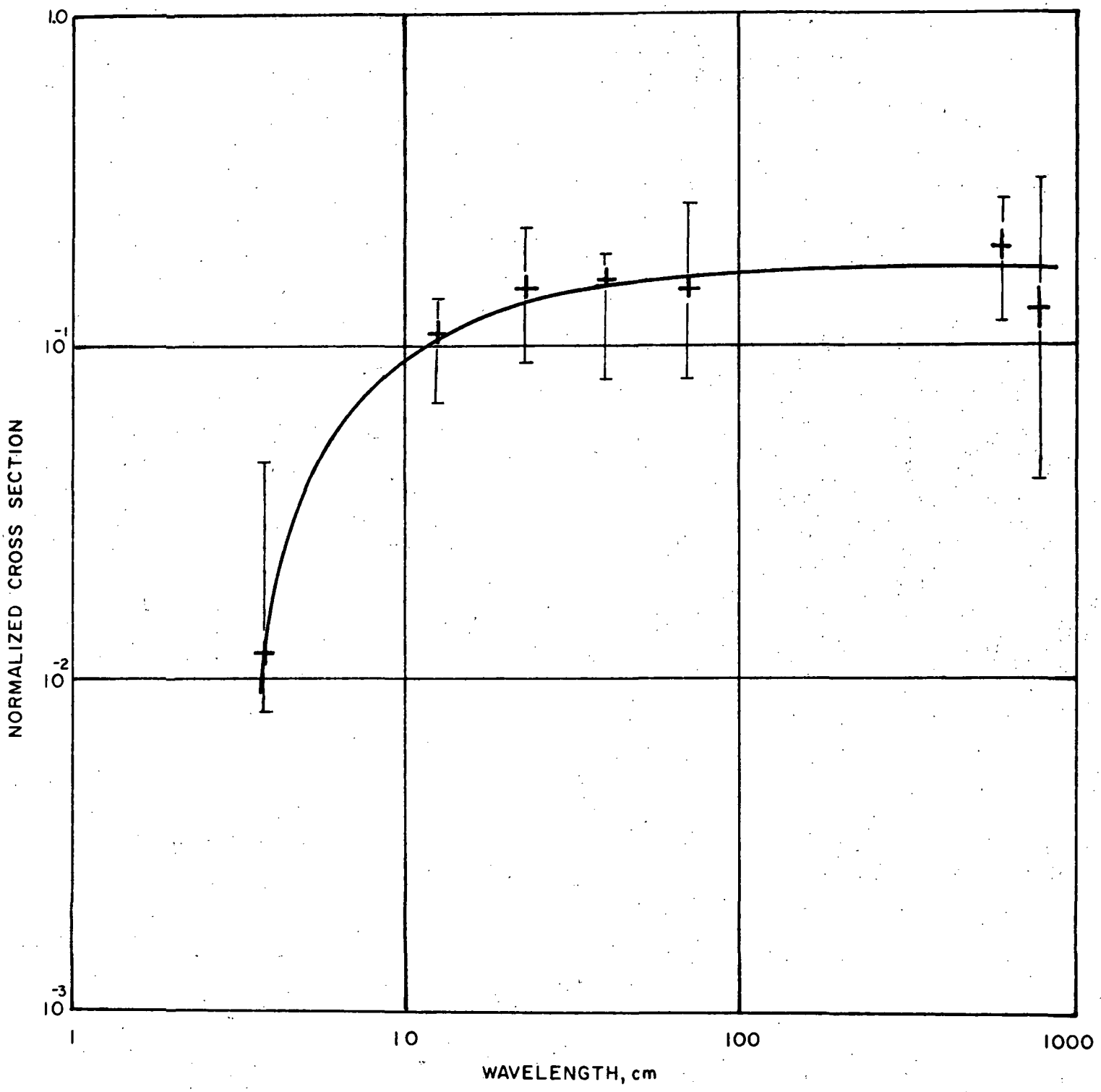

FIGURE 3. NORMALIZED RADAR CROSS SECTION-VENUS

(Goldman and Brandenburg, 1971)

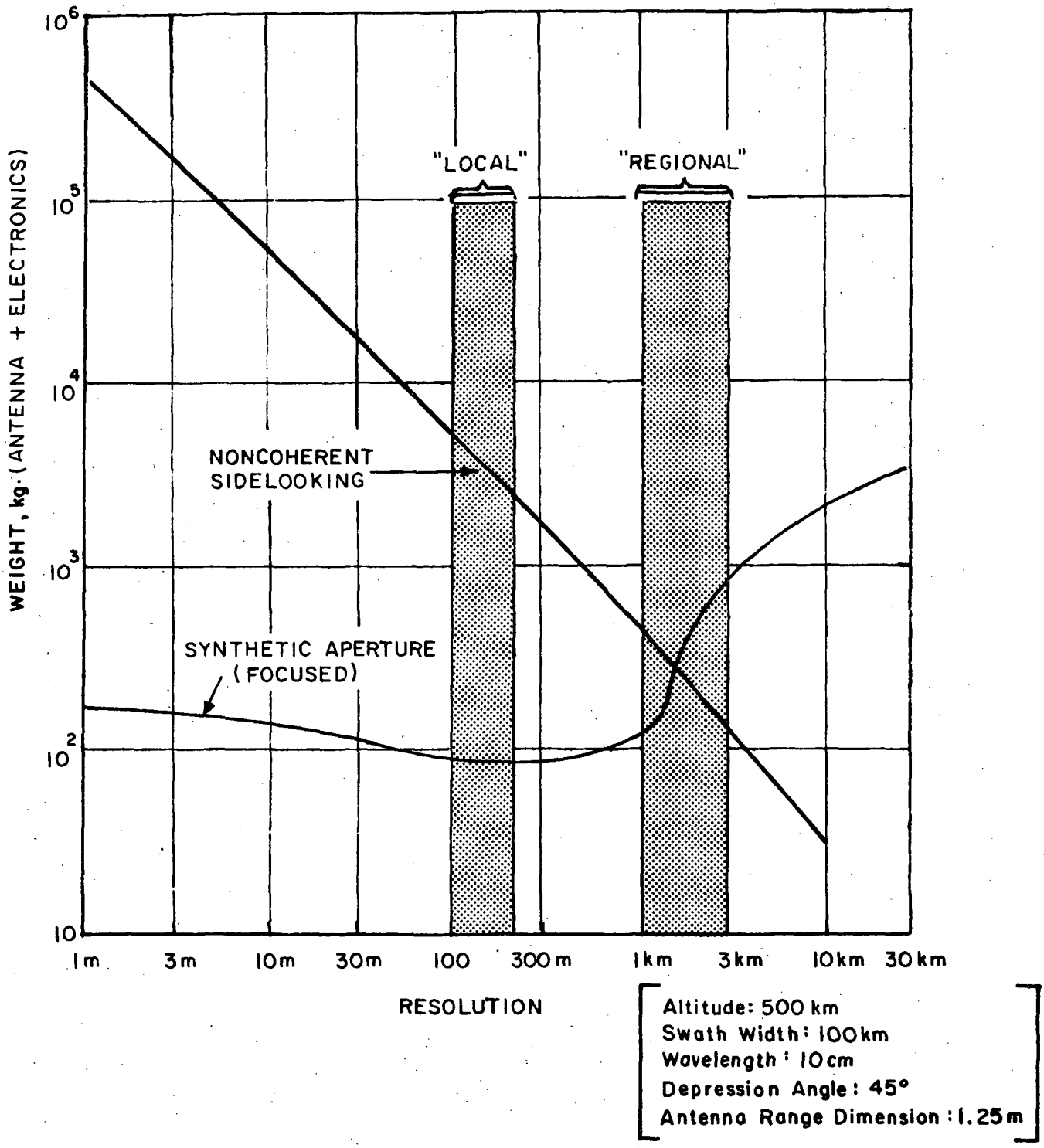

FIGURE 4. COMPARISON OF NONCOHERENT SIDE-LOOKING AND SYNTHETIC APERTURE RADAR SYSTEM WEIGHTS.

antenna weights and do not reflect any data management, power or other systems requirements. The system weights were computed using a method developed in the Klopp study (1969) for a fixed spacecraft orbit (circular-polar). From Figure 4 it appears that the noncoherent system is a good choice if resolutions worse than 1 km are desired. For resolutions under 1 km the synthetic aperture system is obviously preferred.

The choice of which system to investigate at each of the resolution levels of concern in this study is readily apparent from Figure 4. Noncoherent side-looking radar is applicable at the regional level and synthetic aperture at the local level.

2.4 Radar Systems - Parametric Development

In this subsection the system parameters, such as antenna size, power requirements, data acquisition rate, and electronics weight, are developed for the noncoherent and synthetic aperture radar systems. The scaling laws used were derived by Klopp (1969). The effect on the systems due to varying the measurement specifications over those ranges consistent with the definitions of regional and local levels and with varying altitude is shown.

For both systems circular polar orbits with altitudes varying between 300 and 1300 km were used. The polar orbit was chosen to maximize the rate of the planet's apparent rotation under the orbit. (Venus has no known oblateness factor to perturb the orbit.) Circular orbits were used because radar operates most efficiently and at constant resolution over constant altitudes. (Elliptical orbits require varying power levels and antenna orientation for constant resolution throughout the orbit.) A minimum orbital altitude of 300 km was used to avoid atmospheric drag (Uphoff 1970) while a maximum of 1300 km was chosen to provide a range thought to be typical for the two types of radar considered.

2.4.1 Noncoherent Sidelooking Radar Systems Development

Figure 5 illustrates the logic used to size the noncoherent radar system. The four chief input parameters are azimuth, range, vertical resolution and swath width. These four parameters were varied within the limits of the regional level in order to judge their influence on the total radar system. This will become clearer in the following discussion.

2.4.1.1 Antenna Size

The range beamwidth, β_r, of the antenna determines the swath width, W, as shown in Figure 6. Radar map interpretation is aided by having large continuous swath widths. For the regional level a 1000 km swath width might be desirable. To obtain this size swath at a 300 km altitude and 45° depression angle requires a beamwidth of 116°. This covers area directly beneath the spacecraft which cannot be resolved in range. Even decreasing the depression angle α to its minimum value of 18°, so that R_2 just skims the horizon, part of the 1000 km swath still falls beneath the spacecraft. Thus a 1000 km swath width cannot be obtained at 300 km altitude. At 1300 km the 1000 km swath is possible with a beam width of 25° and depression angle of 45°. The relationship between beamwidth β_r (in radians) and antenna range dimension D_r is,

$$D_r = \frac{1.25\ \lambda}{\beta_r} \qquad (2.4)$$

where λ, the wavelength, is 10 cm. The required range dimension at 1300 km is then 29 cm. This is the maximum dimension possible, for as the altitude is decreased the beamwidth becomes larger for a fixed swath width. As will be seen later

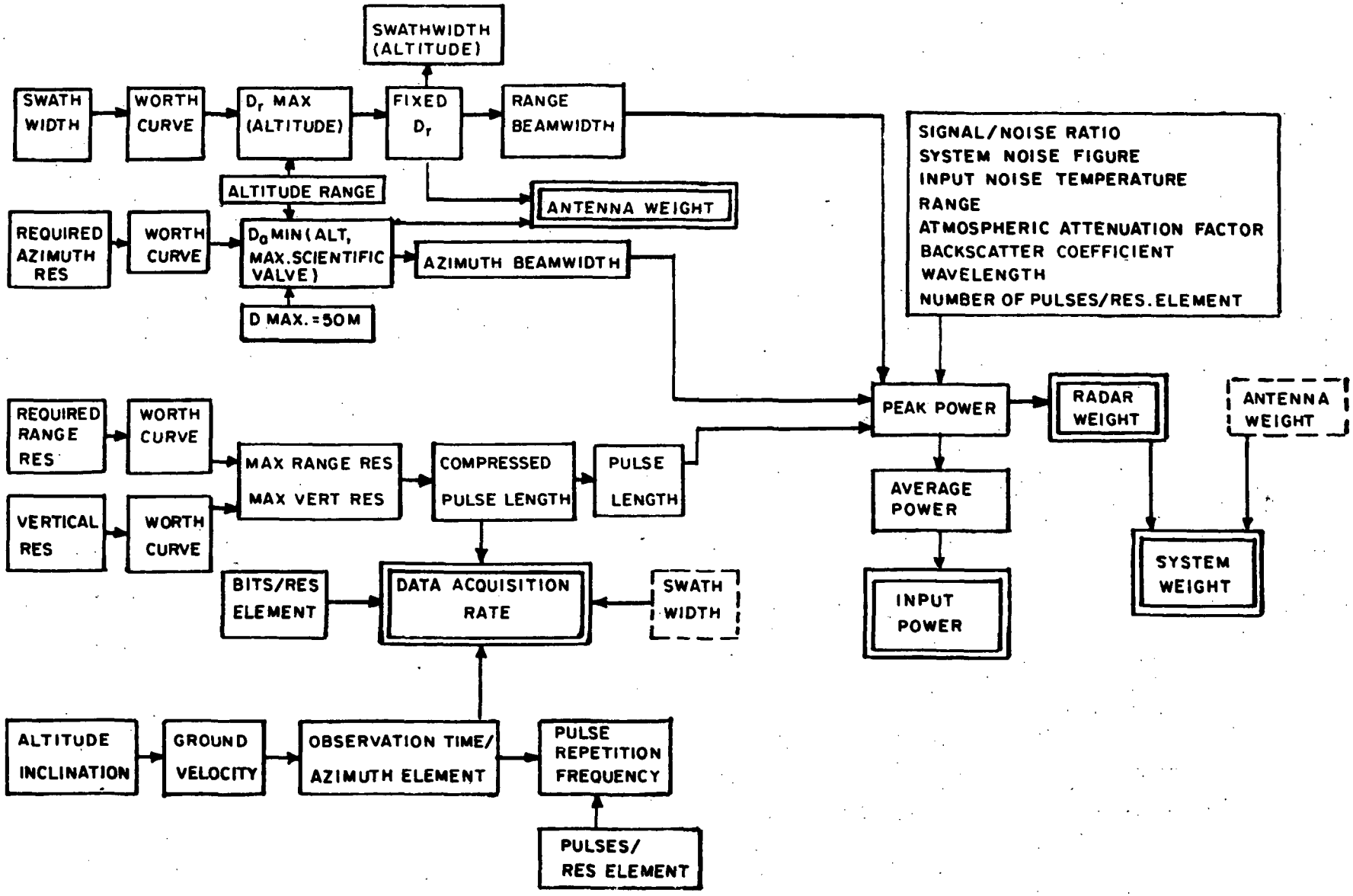

FIGURE 5.

DESIGN LOGIC NONCOHERENT RADAR SYSTEMS

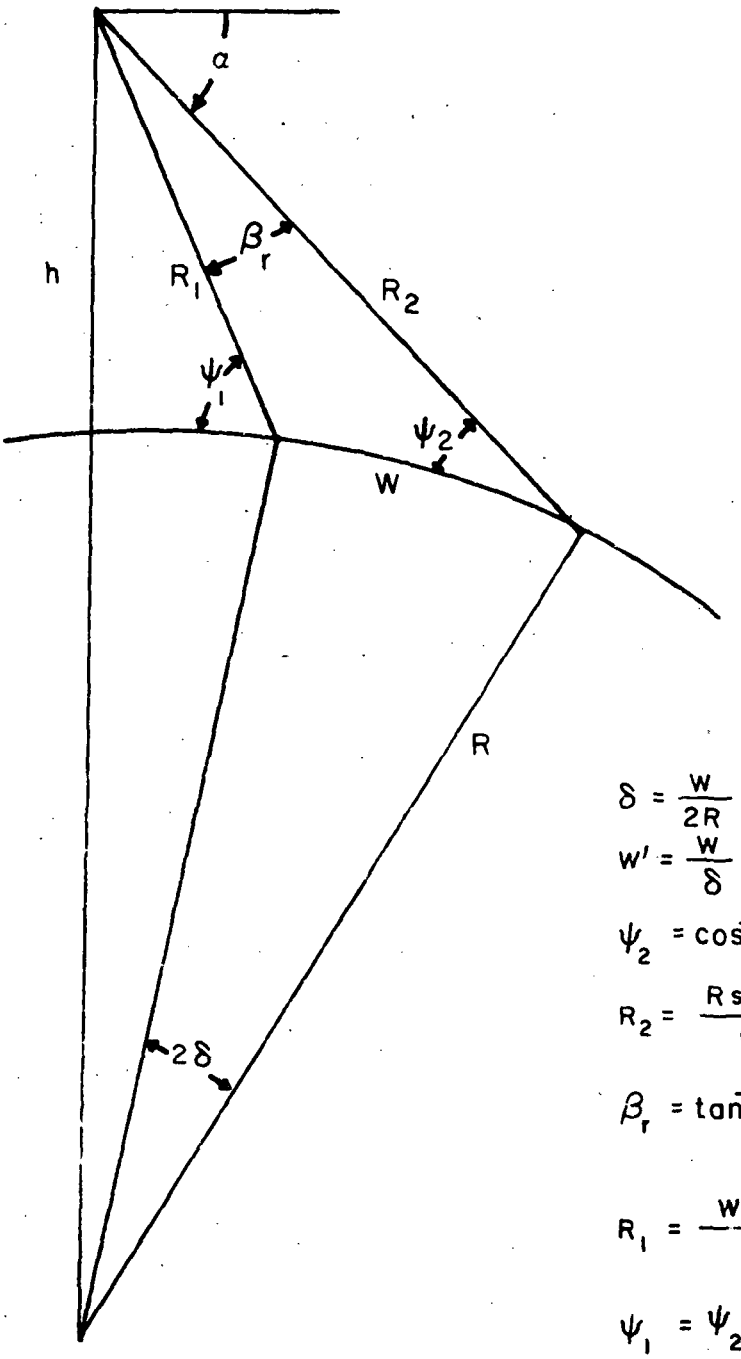

$$\delta = \frac{W}{2R}$$

$$w' = \frac{W}{\delta} \text{ SIN } \delta$$

$$\psi_2 = \cos^{-1}\left(\frac{R+h}{R}\cos\alpha\right)$$

$$R_2 = \frac{R\sin(\alpha - \psi_2)}{\cos\alpha}$$

$$\beta_r = \tan^{-1}\left[\frac{w' \sin(\psi_2 + \delta)}{R_2 - w'\cos(4_2 + \delta)}\right]$$

$$R_1 = \frac{w' \sin(\psi_2 + \delta)}{\sin\beta_r}$$

$$\psi_1 = \psi_2 + \beta_r + 2\delta$$

FIGURE 6. SIDE-LOOKING RADAR GEOMETRY

the azimuth dimension of the antenna ranges between 20 and 50 meters. It is unlikely that antennas 50 meters long and less than a third of a meter wide can be successfully fabricated, folded, deployed, and pointed while keeping a $\lambda/10$ surface accuracy. The swath width requirements may be relaxed in favor of a larger antenna range dimension and structural rigidity.

If the antenna's range dimension is fixed at 1.5 meters the width of the ground swath will range between 50 km and 250 km at altitudes between 300 and 1300 km, respectively. By patching a suitable number of these swaths, correctly overlapped, together a surface map may be built up. This reduction of swath size not only enables a realistic antenna size to be used but also considerably decreases the load on the power and data acquisition subsystems.

The azimuth beamwidth, β_a, is related to the resolution in that dimension, r_a, and the slant range, R_2, by the expression,

$$\beta_a = \frac{0.87\ r_a}{R_2} \tag{2.5}$$

The antenna's azimuth dimension is given by,

$$D_a = \frac{1.25\ \lambda}{\beta_a} \tag{2.6}$$

where λ is equal to 10 cm. Obviously, the smaller the resolution desired the larger D_a must be. Figure 7 illustrates the resolutions achievable with four azimuth dimensions at altitudes between 300 and 1300 km. A 50 m antenna was considered to be the largest which could be used for a spacecraft radar system in this study. Note that 1 and 2 km resolution is achievable only at low altitudes with the largest size antennas.

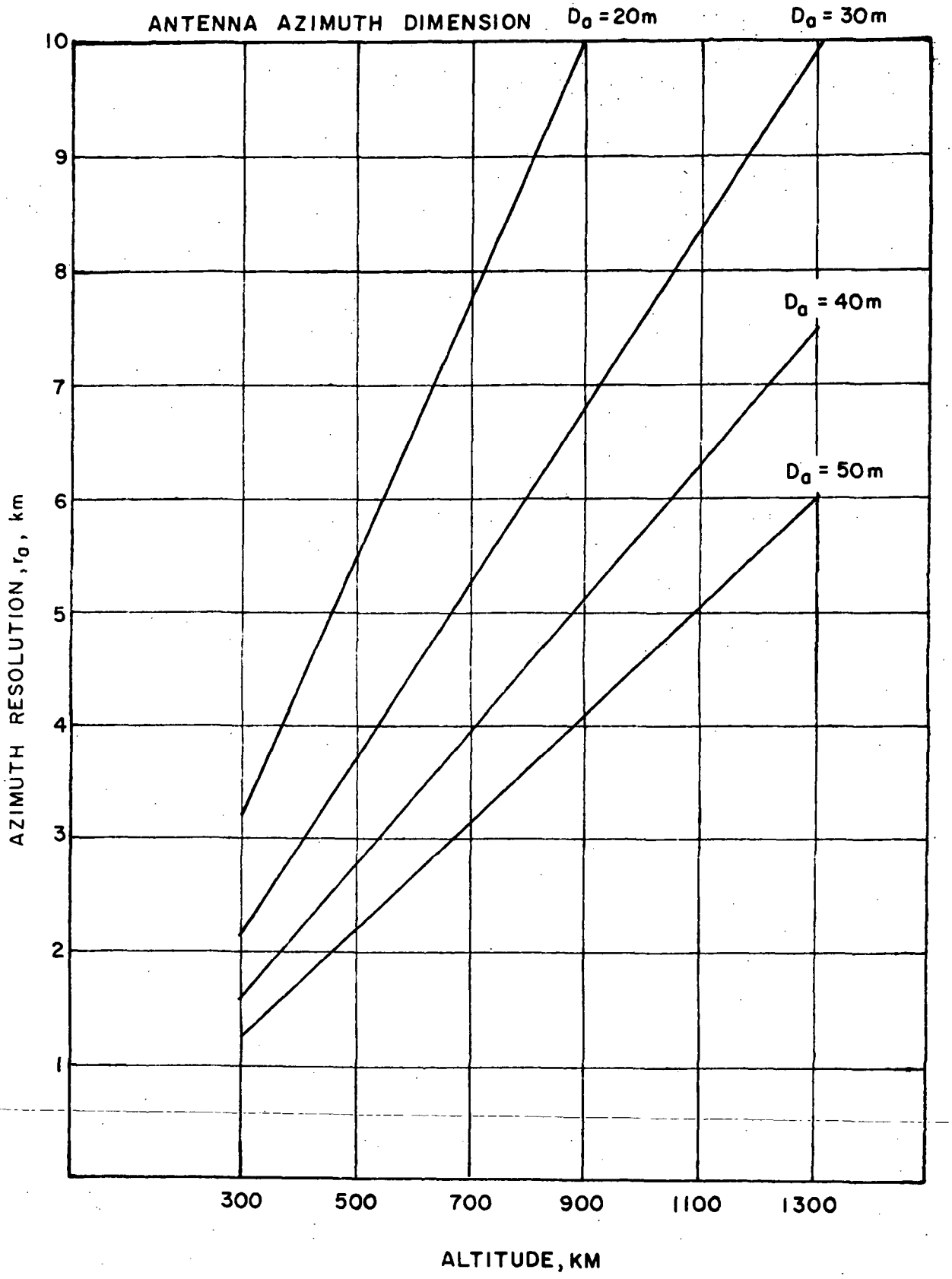

FIGURE 7. AZIMUTH RESOLUTION VS. ALTITUDE AND ANTENNA AZIMUTH DIMENSION (NONCOHERENT SIDELOOKING RADAR)

The procedure employed here was to select the smallest azimuth dimension which provides 3 km. resolution until the 50 m antenna size limit was reached. Figure 8 shows the azimuth dimensions selected and the resolutions they provide. The 50 m size limit is reached at 700 km, and the resolution begins to degrade with increasing altitude until at 1300 km, 6 km azimuth resolution is the best achievable.

The antenna weights, W_A, are given by the relationship

$$W_A = N D_r D_a \qquad (2.7)$$

where D_a is given above, D_r is fixed at 1.5 m and N is the areal density. Little experience exists in large, rectangular, spacecraft antenna design from which to determine representative values for N. Figure 9 shows the results obtained for N as a function of dimension by fitting a second order curve to a number of large antennas designed at JPL (Heer and Yang 1971). Using the appropriate values of N the 1.5 x 21.5 m antenna weighs 59 kg, the 1.5 x 37 m, 131 kg and the 1.5 x 50 m, 200 kg.

2.4.1.2 Pulse Length

The range and vertical resolutions are determined by the pulse length, τ. Range resolution is given approximately by

$$r_r \cong \frac{c\tau}{2 \cos \psi}$$

where c is the speed of light and ψ is an average grazing angle. Note that the range resolution is directly affected by the length of the pulse. Pulse compression techniques allow a long pulse to be transmitted with the returning echo processed so that the effective or compressed pulse length, τ_c, is much

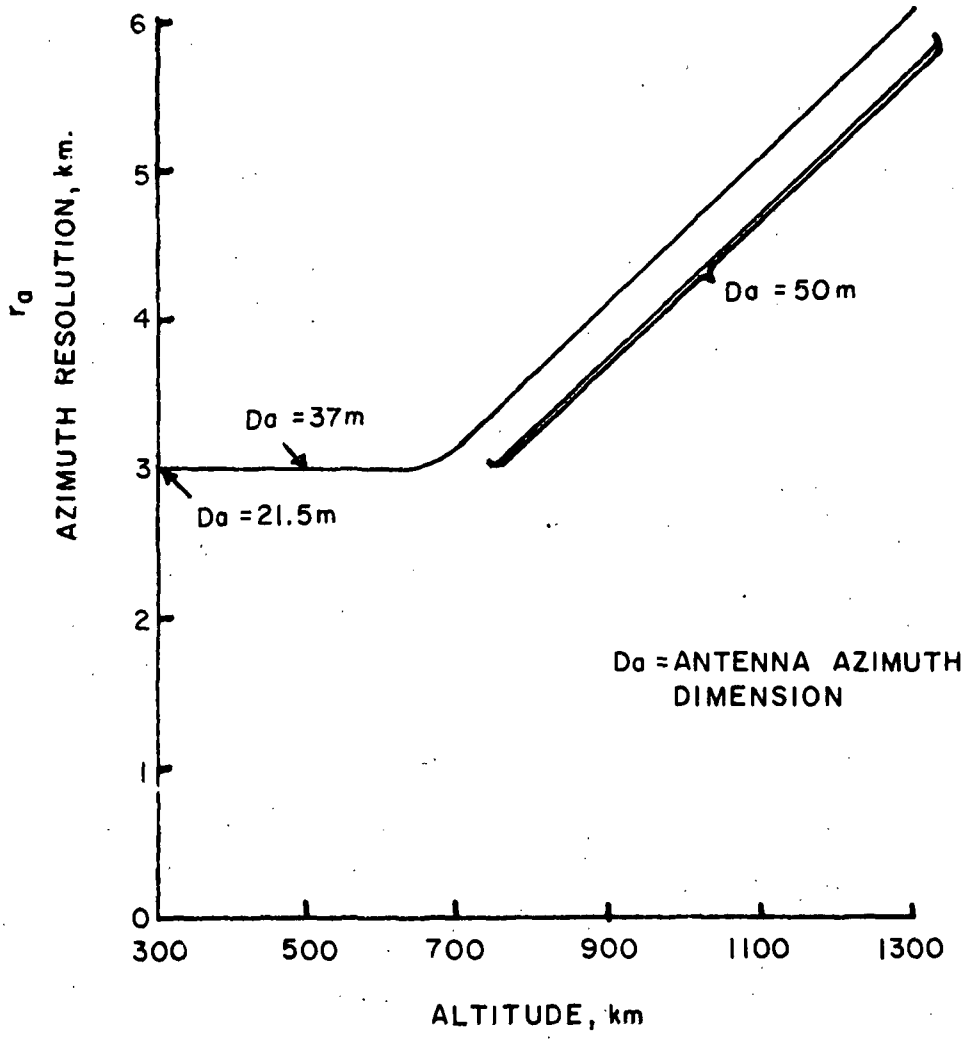

FIGURE 8. AZIMUTH RESOLUTIONS ACHIEVABLE -NONCOHERENT SIDE-LOOKING RADAR.

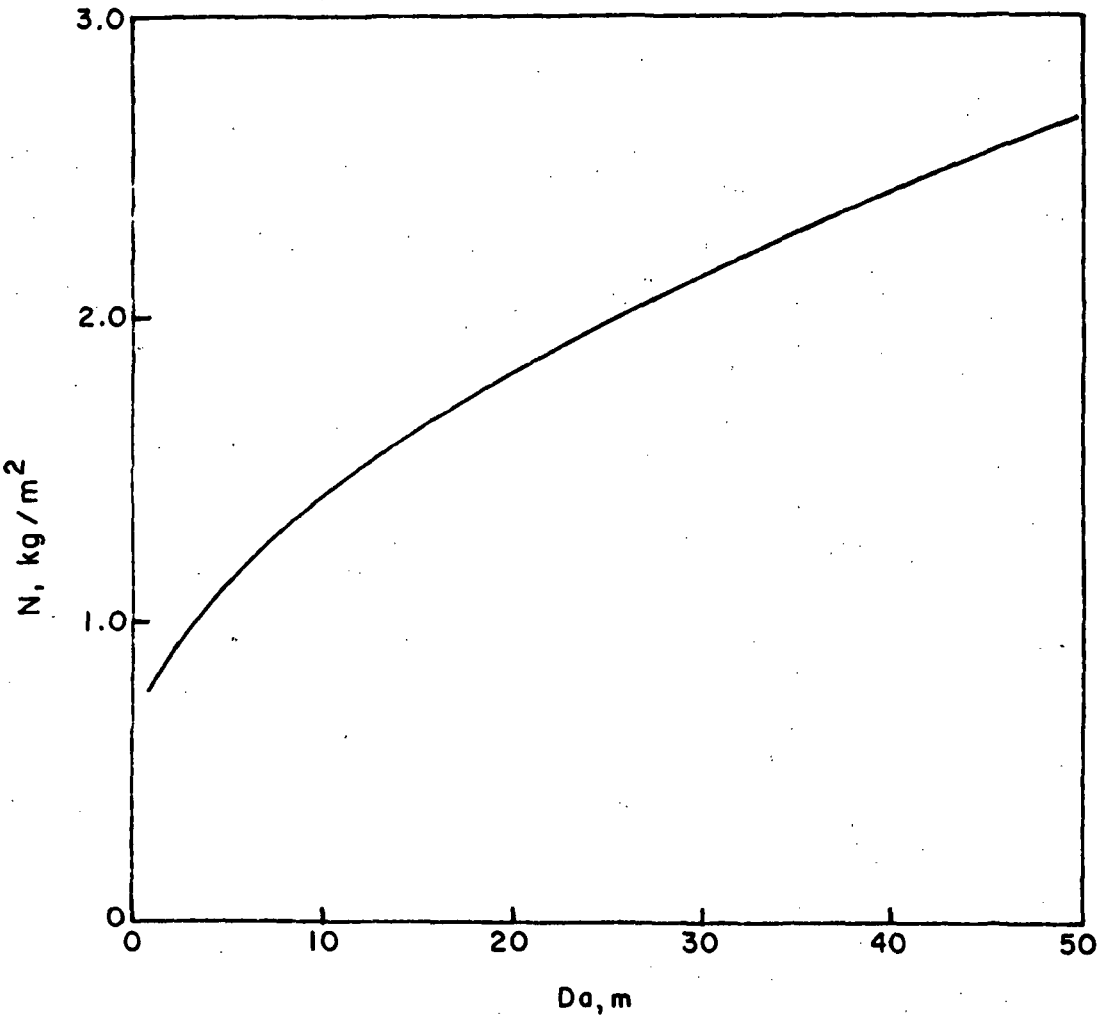

FIGURE 9. ANTENNA DENSITY AS A FUNCTION OF LENGTH.

shorter than the transmitted pulse. A pulse compression ratio, τ/τ_c, of 200 was used here.

The compressed pulse is constrained by,

$$3.33 \times 10^{-9} \text{ sec} \leq \tau_c \leq \frac{2\, r_r \cos \psi_1}{c} \text{ sec} \qquad (2.8)$$

for a wavelength of 10 cm, and ψ_1 is the grazing angle at the near edge of the swath (Klopp, 1969). The inequality on the left hand side is derived from constraining the receiver bandwidth to 10 percent or less of the operating frequency.

The range and vertical resolutions are related by,

$$r_r = \frac{r_v}{\tan \psi_1} \text{ (see Fig. 6)} \qquad (2.9)$$

In order to achieve vertical resolutions of about 1 km (regional) at a 45° depression angle (α) the range resolution must also be about 1 km. Since the azimuth resolution is 3 km or worse the ground resolution elements, $r_a \times r_r$, are rectangular. Hence it is necessary, therefore, to design for a fixed set of vertical resolutions. Figure 10 illustrates the relationship between range resolution, vertical resolution and altitude.

Taking vertical resolutions between 0.5 and 1 km as the most desirable for the regional level, the associated pulse lengths may be computed. Figure 11 shows the compressed and actual pulse lengths which must be used to obtain these vertical resolutions.

2.4.1.3 Pulse Repetition Frequency (PRF)

The pulse repetition frequency, the number of pulses radiated each second, is dependent chiefly on the number of pulses desired per resolution element, m, and the length of time, t_o, that the radar beam dwells on an azimuth resolution

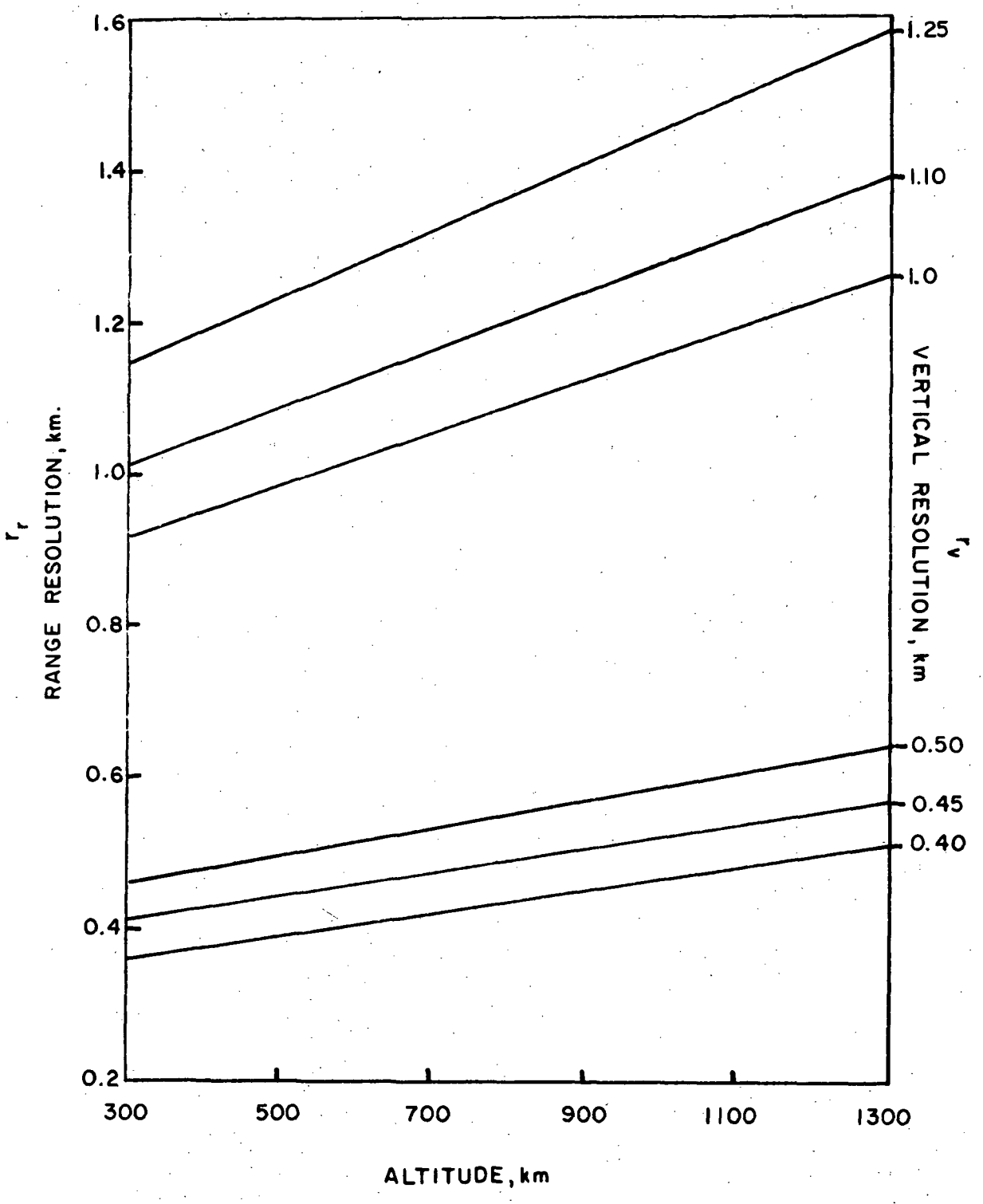

FIGURE 10. RANGE AND VERTICAL RESOLUTION VS. ALTITUDE
(D_r = 1.5m, α = 45°, λ = 10cm)

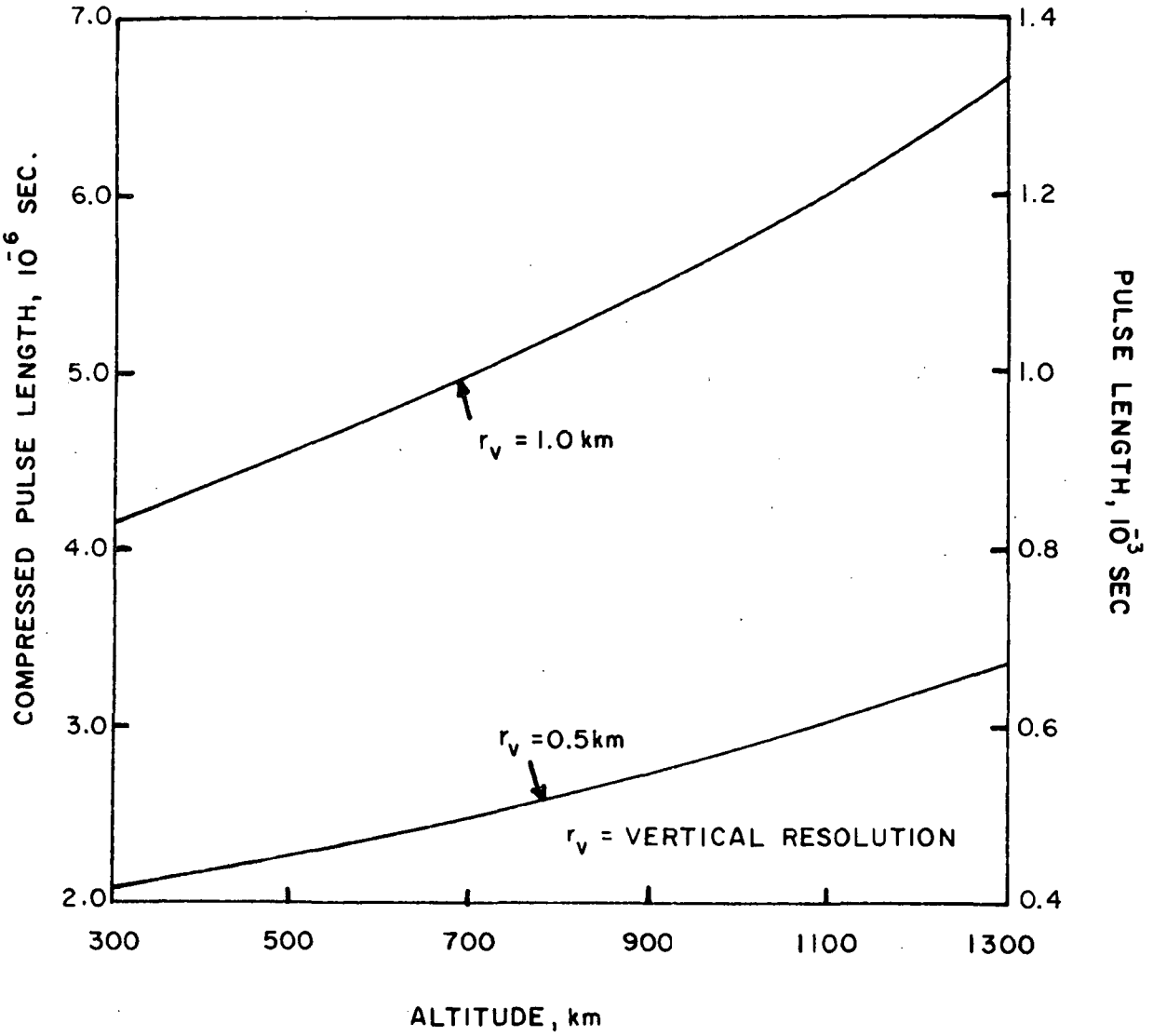

FIGURE 11. PULSE LENGTH VS. ALTITUDE
($\alpha = 45°$, $\lambda = 10cm$)

element. The power contained in the pulse is inversely proportional to the square root of the number of pulses analyzed per resolution element. In this respect it is advantageous to use a large m. However, the average power that must be fed to the radar system is directly proportional to m. These two considerations tend to balance each other; m is often chosen as unity.

The minimum time, t_o, that a target resolution element will spend within the radar beam is,

$$t_o = \frac{2\,R}{v_h} \sin^{-1}\left[\frac{R_1 \sin(\beta_a/2)}{h + R - R_1 \sin(\alpha+\beta_r)}\right] \qquad (2.10)$$

where R_1 is the slant range to the near edge of the swath (see Fig. 6), β_a is given by Equation 2.5, $\alpha = 45°$, and $\beta_r = 4.75°$. v_h is the spacecraft's horizontal ground velocity, and is given by,

$$v_h = \frac{R}{R + h}\left[\frac{3.25 \times 10^{14}}{R + h}\right]^{1/2} \qquad (2.11)$$

for circular orbits where R and h are expressed in meters, (Venus' surface rotational velocity is extremely low and has been neglected here.)

If one pulse (m) is to be transmitted every t_o seconds, then the pulse repetition frequency, p, is

$$p = 1/t_o \qquad (2.12)$$

Table 1 lists the values of v_h, t_o, and p used in this section. t_o and p are constant up to 700 km altitude because the azimuth beamwidth is decreasing (D_a increasing) at a rate which effectively cancels out the decreasing ground velocity's effect.

TABLE 1

VARIATIONS OF GROUND VELOCITY, OBSERVATION TIME, AND PULSE REPETITION FREQUENCY WITH ALTITUDE

Altitude, h	Ground Velocity, V_h	Observation Time, t_o	Pulse Repetition Frequency, p
300 km	6.8 km/sec	0.41 sec	2.44 pulses/sec
500	6.5	0.41	2.44
700	6.2	0.41	2.44
900	5.9	0.54	1.86
1100	5.7	0.65	1.54
1300	5.5	0.73	1.37

$\alpha = 45°$

$\beta_r = 4.75°$

2.4.1.4 Power

The peak transmitted power for noncoherent radar systems can be expressed as,

$$P_t = \frac{10^{-30} \, (S/N) \, F_o \, T \, R_2^{\,3} \, \beta_a \, \beta_r^{\,2} \, A \cos \psi_2}{\tau \, \tau_c \eta \, m^{1/2} \, \lambda^2} \qquad (2.13)$$

where:

S/N = signal to noise ratio = 10
F_o = system noise figure = $\exp[3.8 - .344 \ln(100\lambda)] = 20.24$
T = input noise temperature = 700° K for Venus
R_2 = slant range to far edge of swath (see Fig. 6)
β_a = azimuth beamwidth (see Section 2.4.1.1)
β_r = range beamwidth = 4.75°
A = atmospheric attenuation factor = $\exp (6.5 \times 10^{-4} / \lambda^2 \sin \psi_2) \approx 1.1$
τ = pulse length (see Section 2.4.1.2)
τ_c = compressed pulse length
m = pulses per azimuth element
λ = wavelength = 10 cm

The backscatter coefficient, η, was estimated to be $\sim 5 \times 10^{-4}$ for a 10 cm wavelength and 45° depression angle (Evans and Hagfors 1968).

The variation of the required peak power with altitude is shown on Figure 12. These peak power requirements are not very stringent, being less than 1000 watts for a burst of about 6.5 microseconds.

The average power, $\overline{P}$, is given by the relationship,

$$\overline{P} = \frac{m \tau P_t}{t_o} = p \tau P_t \qquad (2.14)$$

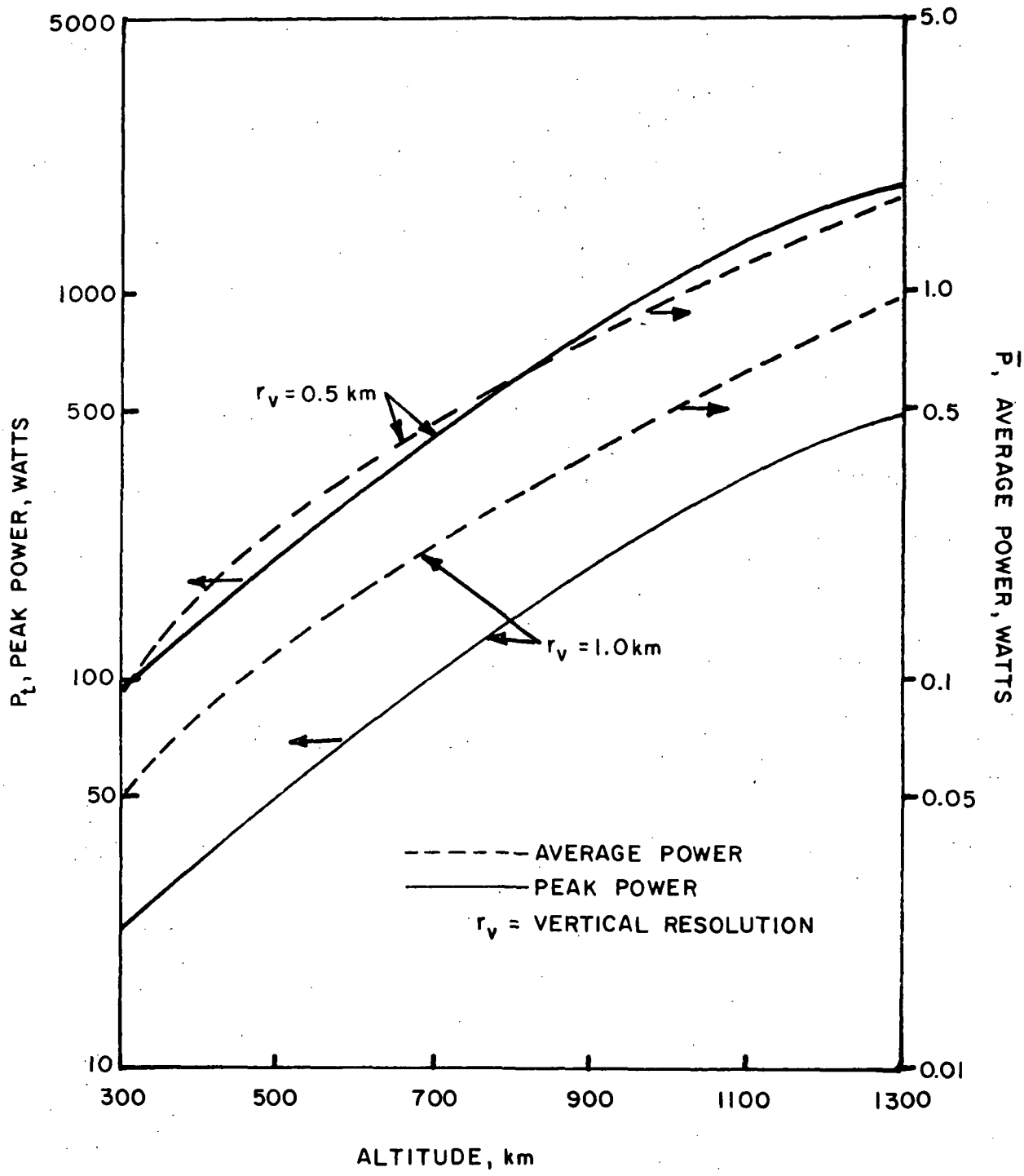

FIGURE 12. PEAK AND AVERAGE POWER VS. ALTITUDE. (NONCOHERENT SIDE-LOOKING RADAR)

where P_t is peak power. The average power requirements are also shown on Figure 12 (right ordinate). The average power is always less than two watts.

The operational power requirements of the radar system, the input power, P_{in}, may be scaled as a function of average power,

$$P_{in} = 100 + 3\ \overline{P}\ \text{watts} \qquad (2.15)$$

Thus for the cases considered here an input power of 106 watts is sufficient for the noncoherent radar system at altitudes up to 1300 km.

2.4.1.5 Weight

The weight, W_r, of the radar electronics is best expressed as a function of the peak power generated (Klopp, 1969).

$$W_r = 13.6 + 9.1\ \ln\ (0.1\ P_t\ \lambda)\ \text{kg}. \qquad (2.16)$$

where 13.6 kg is the minimum weight. The weights of the radar electronics for the range of altitudes between 300 and 1300 km and the two values of vertical resolution used are given in Table 2.

The total radar system weight is the sum of the electronics weight and the antenna weights, given at the end of Section 2.4.1.1. The total system weight is shown in Figure 13. The antenna weights tend to dominate the system, especially at the higher altitudes. The bend in the curves is caused by a constant antenna size (1.5 x 50 m) above 700 km.

TABLE 2

RADAR ELECTRONICS WEIGHT

Altitude, km	Electronics Weight, kg	
	r_v* = 0.5 km	r_v = 1.0 km
300	13.6	13.6
500	20.8	13.6
700	26.3	13.8
900	31.4	18.7
1100	36.9	24.3
1300	40.2	27.8

* r_v = Vertical Resolution

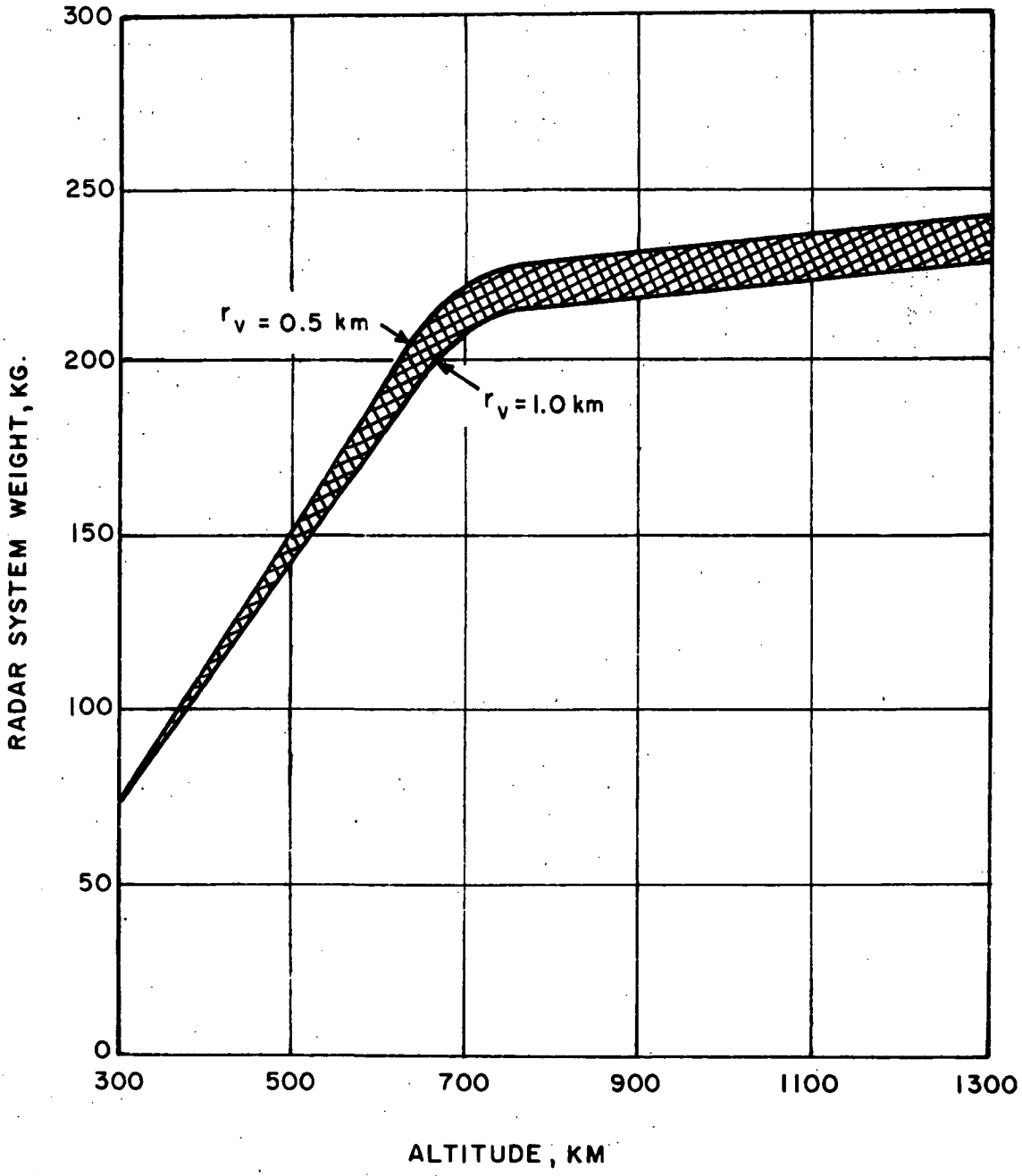

FIGURE 13. TOTAL RADAR SYSTEM WEIGHT (ANTENNA & ELECTRONICS) NONCOHERENT SIDE-LOOKING RADAR.

2.4.1.6 Data Acquisition

The data acquisition rate, DR, is the last parameter to be determined. A good approximation to this data collection rate, where each resolution element is described by G binary bits, is,

$$DR \cong \frac{WG}{c\,\tau_c\,t_o}\,(\cos\psi_1 + \cos\psi_2) \qquad (2.17)$$

where all terms were defined previously (see Figure 6). Setting G equal to six bits per resolution element, the data acquisition rate is shown as a function of altitude in Figure 14. The curves flatten out and begin falling off at about 700 km altitude. Once again this is due to the constraint on antenna size. Although the swath width continues to increase with altitude the size of the resolution element decreases more rapidly beyond 700 km, with the net result that the radar views fewer resolution elements per unit time.

2.4.1.7 Noncoherent Radar Systems - Summary

Noncoherent side-looking radar systems operating with a depression angle of 45° at a wavelength of 10 cm, in circular polar orbits between altitudes of 300 and 1300 km at Venus and mapping at the regional level, have requirements which appear to be reasonable in terms of spacecraft design. The antenna must be between 21.5 m and 50 m in length and 1.5 m wide, which may present some problems. The peak and input powers range between 20 and 2000 watts and 100 and 106 watts, respectively, and should not be any burden to present power systems. The total system weights, 75 to 250 kg, are not too high for integration into a spacecraft and the data acquisition rates,

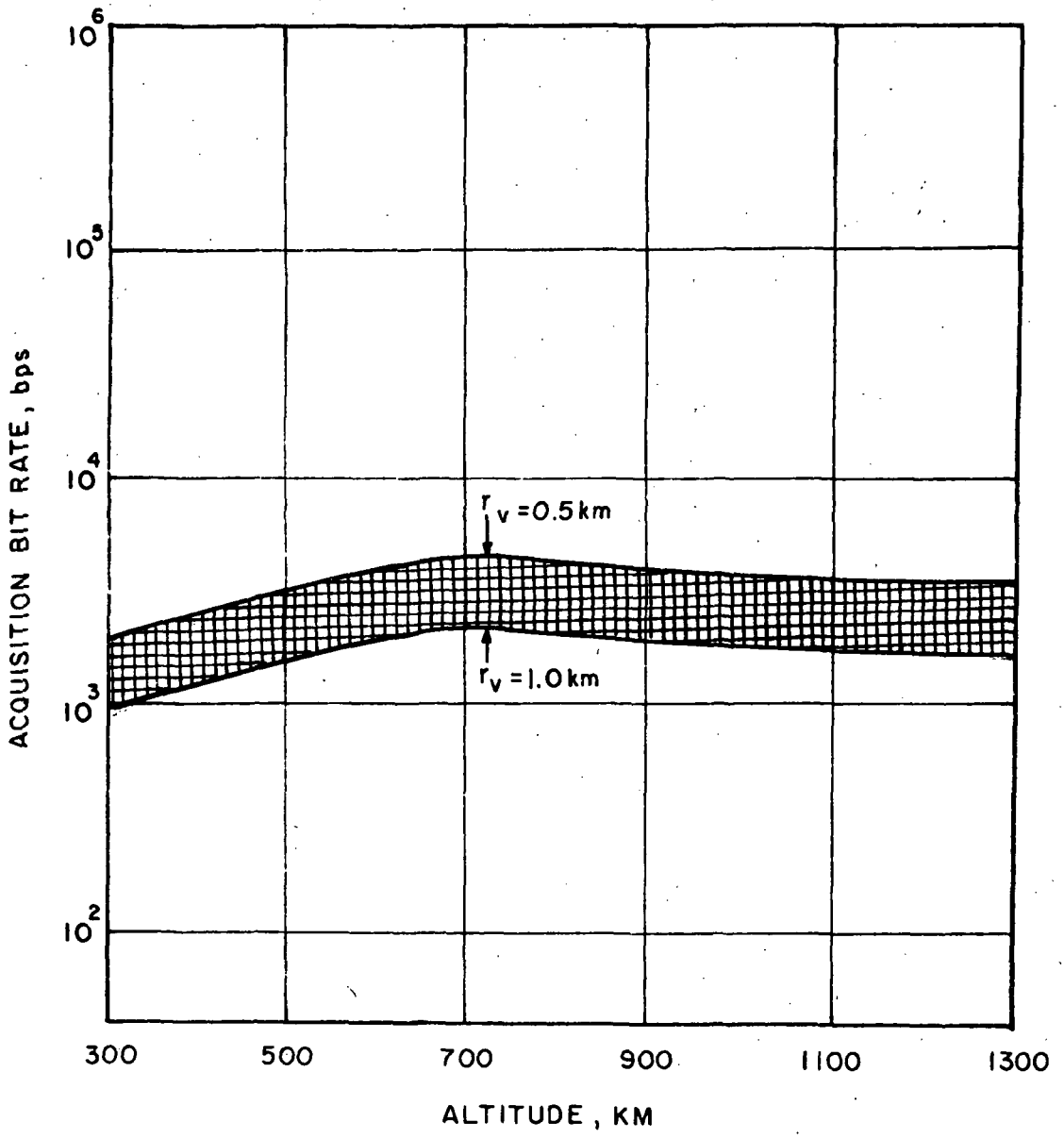

FIGURE 14. ACQUISITION BIT RATE NONCOHERENT SIDE-LOOKING RADAR (6 BITS/RESOLUTION ELEMENT)

1000 - 4400 bps, can easily be handled by current systems. The actual spacecraft sizing is described in Section 3, but the large antenna length is the only significant problem seen to hamper the use of noncoherent radar for regional Venus mapping.

2.4.2 Focused Synthetic Aperture Radar Systems Development

Synthetic aperture radar was selected to cover the local scale of resolutions and coverage described in Section 1. The radar system scaling that follows will therefore be aimed at ground resolutions of about 100 m and swath widths of about 100 km.

Figure 15 illustrates the logic used to size the synthetic aperture radar system. Here the three chief input parameters are ground resolution, vertical resolution, and swath width size. As was seen in Section 2.1 a square ground resolution element is obtainable with synthetic aperture radar, where it was not with noncoherent. Range resolution is specified in Figure 15, but range and azimuth resolution may be used interchangeably as they are equal.

2.4.2.1 Pulse Length

The range and vertical resolutions are related through shadowing in the same manner as for noncoherent radar. Recall equation 2.9,

$$r_r = \frac{r_v}{\tan \Psi_1}$$

where r_r is the range and r_v is the vertical resolution. For synthetic aperture radar the range and azimuth resolutions are conveniently selected as equal, so the vertical resolution is

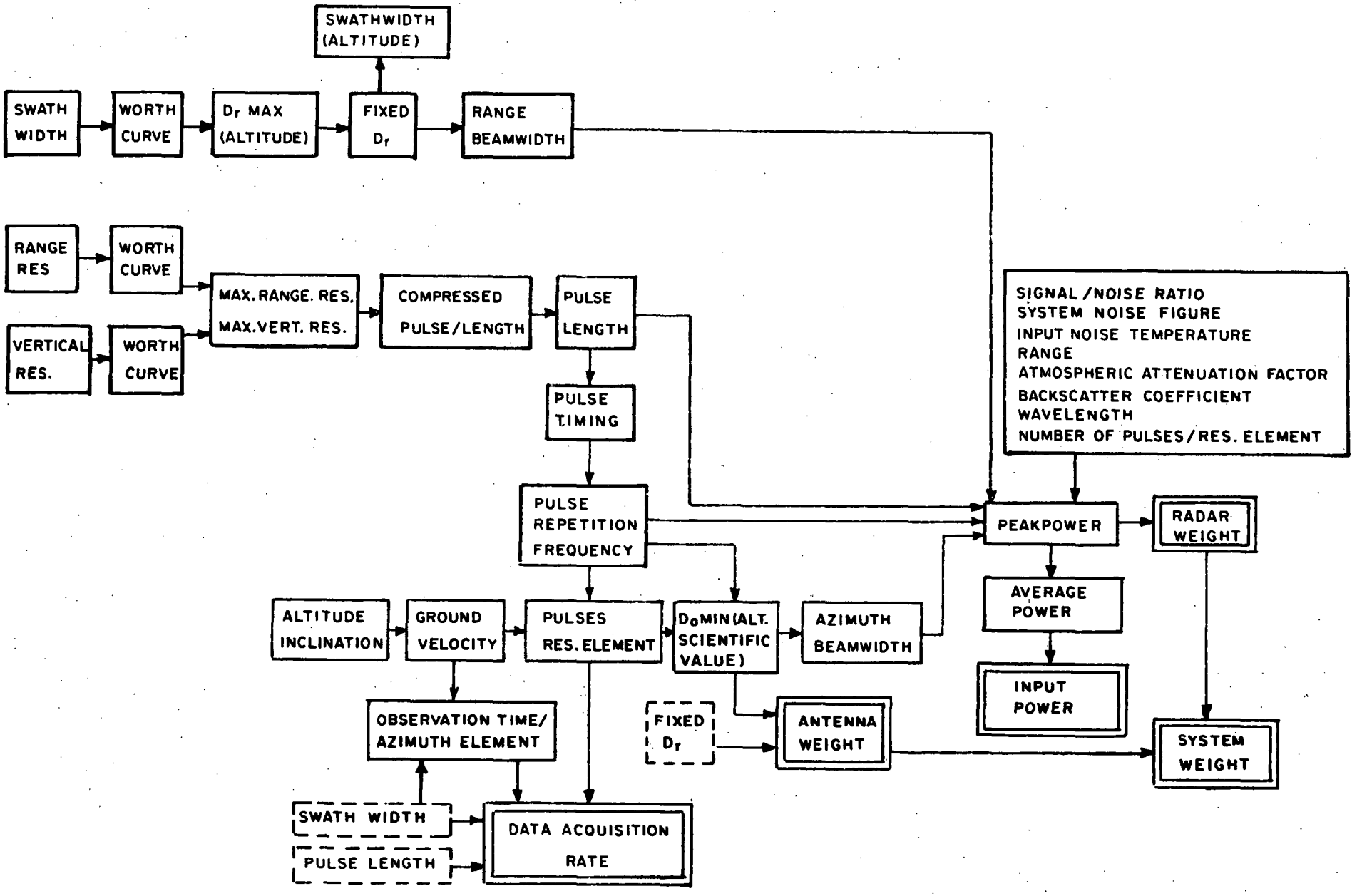

FIGURE 15. DESIGN LOGIC FOCUSED SYNTHETIC APERTURE RADAR SYSTEMS

allowed to float, while the ground resolution (r_a, r_r) is fixed. (Vertical resolution was allowed to float for the noncoherent system, while only range resolution was fixed). The synthetic aperture radar system is scaled to provide ground resolutions in the 100 to 200 meter range.

The compressed pulse length, τ_c, is constrained by the same conditions as noncoherent radar,

$$3.33 \times 10^{-9} \text{ sec} \leq \tau_c \leq \frac{2\, r_r \cos \Psi_1}{c} \text{ sec}$$

where the terms have been previously defined. Figure 16 illustrates the variation in the compressed and actual pulse lengths as a function of altitude for 100 and 200 m ground resolutions, using a pulse compression ratio of 200. Vertical resolution varies from 1.1 r_r at 300 km to 0.73 r_r at 1300 km since Ψ_1 remains close to 45°.

2.4.2.2 Pulse Repetition Frequency (PRF)

For the noncoherent radar system it was practical to transmit just one pulse for each azimuthal resolution element and base the pulse repetition frequency accordingly. This is not the case however for the synthetic aperture system, where the effective (generated) length of the aperture (and thus the ground resolution) is based on the number of pulse returns from each azimuth resolution element. In order to keep the actual physical antenna aperture small it is necessary to use the highest prf possible. For the case studied here the maximum prf is obtained if the time between the end of the pulse transmission and the beginning of the sidelobe return (from the subspacecraft point) is used to receive the swath return from the previous pulse. The pulse repetition frequency is then,

$$p \leq \frac{c}{2\,(R_2 - R_1) + c\tau} \qquad (2.18)$$

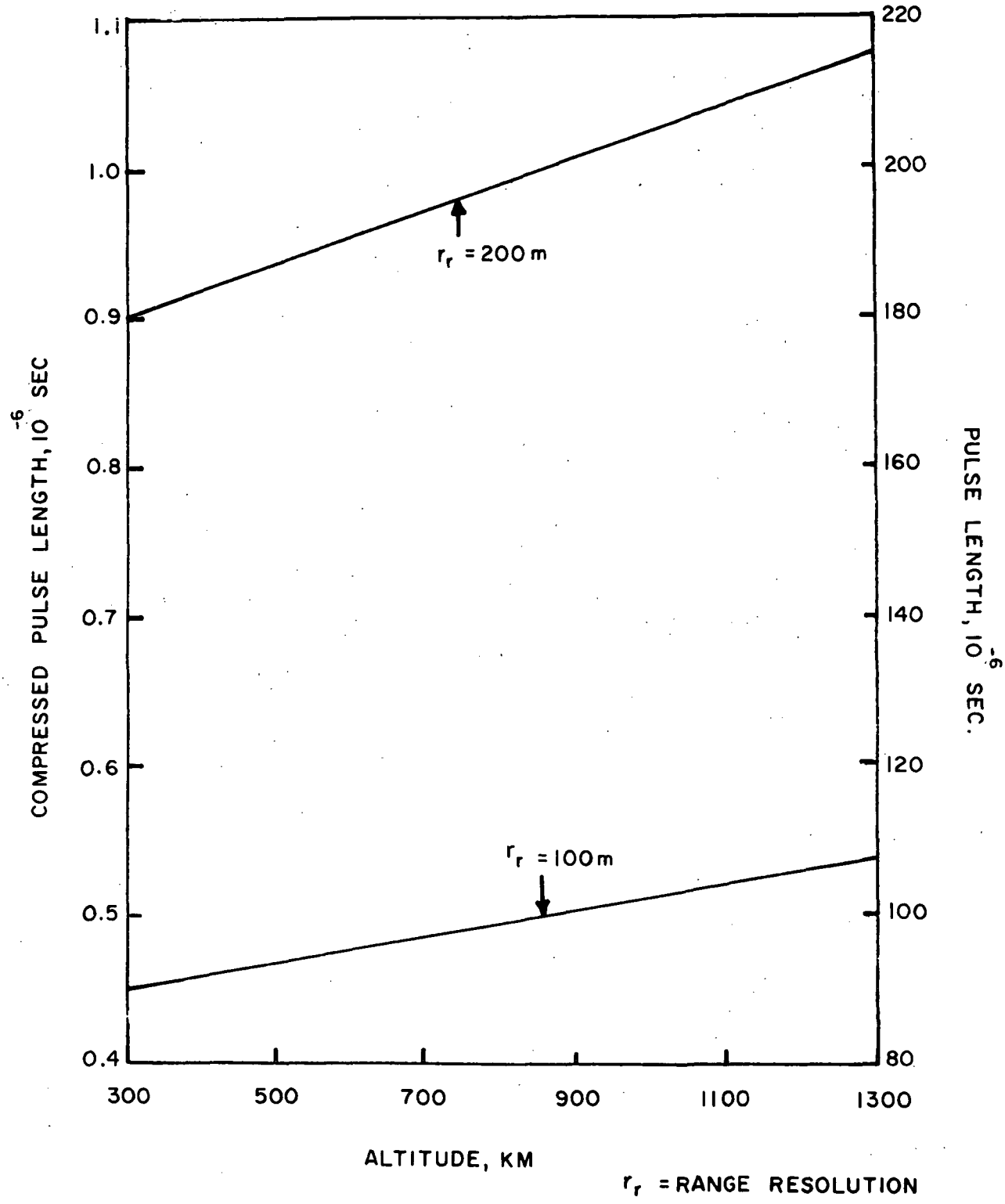

FIGURE 16. PULSE LENGTH VS. ALTITUDE ($\alpha = 45°$, $\lambda = 10$cm) SYNTHETIC APERTURE RADAR

The change in the prf with altitude is shown for 100 m and 200 m resolution in Figure 17.

2.4.2.3 Antenna Size

The swath width of the synthetic aperture system is dependent on the range beamwidth and antenna dimension in exactly the same manner as for noncoherent radar. Once again a 1.5 m range dimension is used, which provides swath widths between 50 and 250 km at altitudes between 300 km and 1300 km, respectively. However, these swath widths are in keeping with the coverage specifications of local mapping.

The azimuth beamwidth, β_a, is related to the antenna's azimuth dimension, D_a, by,

$$D_a = \frac{1.25\ \lambda}{\beta_a}$$

Angular ambiguities will result during the creation of the synthetic aperture if the sidelobe of the synthetic aperture gain pattern does not fall outside the main lobe of the real aperture. This results if the distance the real aperture travels between pulses is too large compared to the actual physical length of the aperture. These ambiguities may be avoided if,

$$D_a \geq \frac{4\ v_h}{p}$$

where v_h is the ground velocity given by equation 2.11 and listed in Table 1. The maximum antenna length is constrained by the need to transmit and receive m pulses from a target while it passes through the beam. This is expressed by,

$$D_a \leq \frac{1.25\ p\ \lambda\ R_2}{m\ v_h} \qquad (2.20)$$

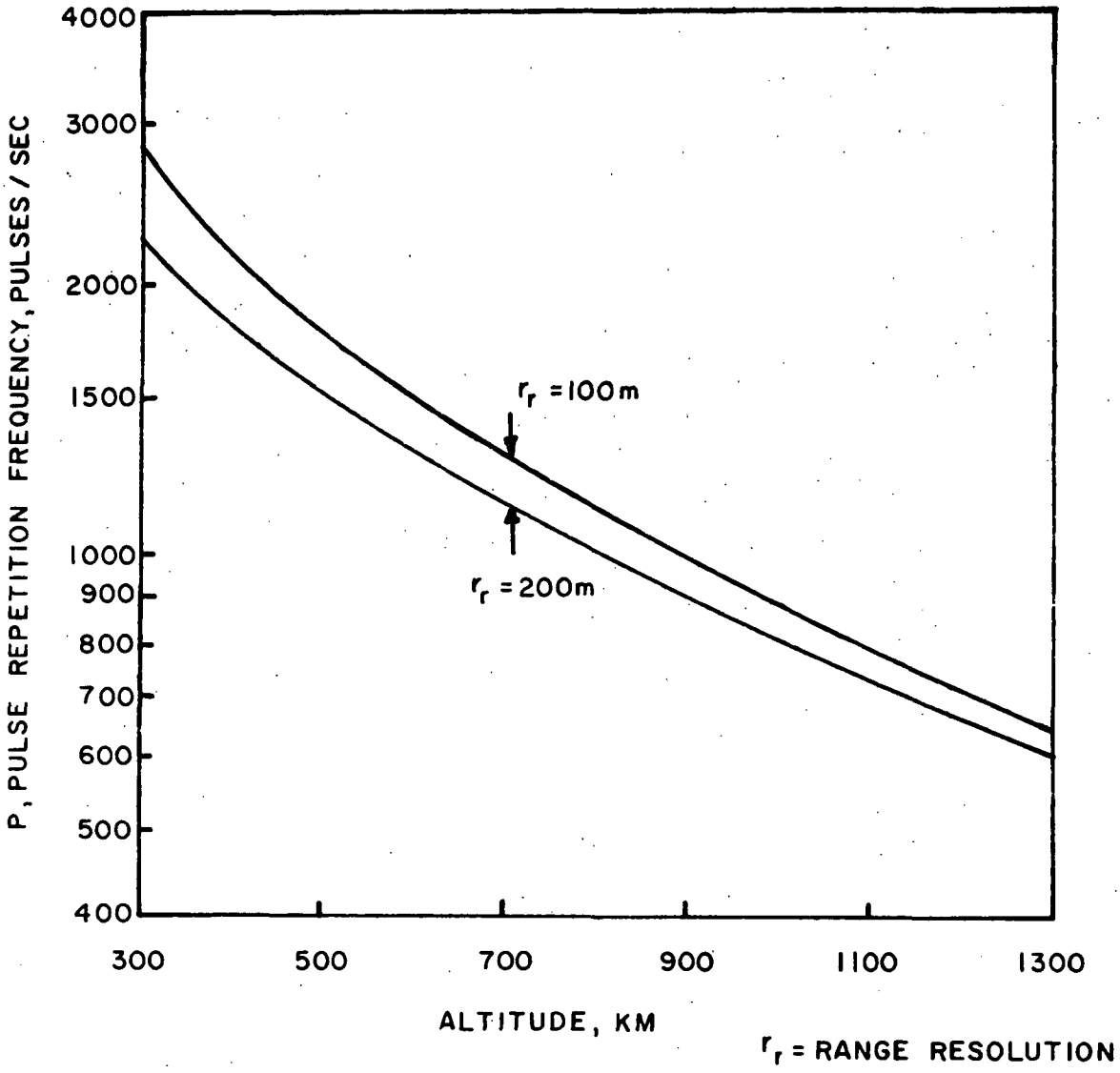

FIGURE 17. PULSE REPETITION FREQUENCY VS. ALTITUDE SYNTHETIC APERTURE RADAR (λ=10cm, α=45°)

where

$$m \geq \frac{p \lambda R_2}{2 r_h v_h} \tag{2.21}$$

Since the average power is directly proportional to m (Eqn. 2.14), it is best to use the minimum value of m to keep the power consumption as low as possible. This does cause the antenna to be larger than optimum, but not as large as for the noncoherent system. The values of m used are shown on Figure 18.

Combining the constraints of equations 2.19 and 2.20, the minimum antenna azimuth dimensions are shown as a function of altitude on Figure 19. Using the scaling law for antenna densities developed in Section 2.4.1.1, the synthetic aperture antenna weights are also illustrated in Figure 19. Notice, that although these antennas are large, between 10 and 35 m, they are considerably smaller than those necessary for noncoherent radars providing resolutions an order of magnitude worse. Note also that the better resolution (100 m) case requires a smaller antenna than the poorer case (200 m). This is one of the attractive aspects of synthetic aperture radar; the size of the resolution element is directly proportional to the length of the antenna, just the opposite of the noncoherent system.

2.4.2.4 Power

The peak power, P_t, contained within the pulse envelope for the synthetic aperture system may be expressed as,

$$P_t = \frac{2.35 \times 10^{-30} (S/N) F_o T v_h R_2^3 \beta_a^2 \beta_r^2 A \cos \Psi_2}{p \tau \tau_c \eta \lambda^3} \tag{2.22}$$

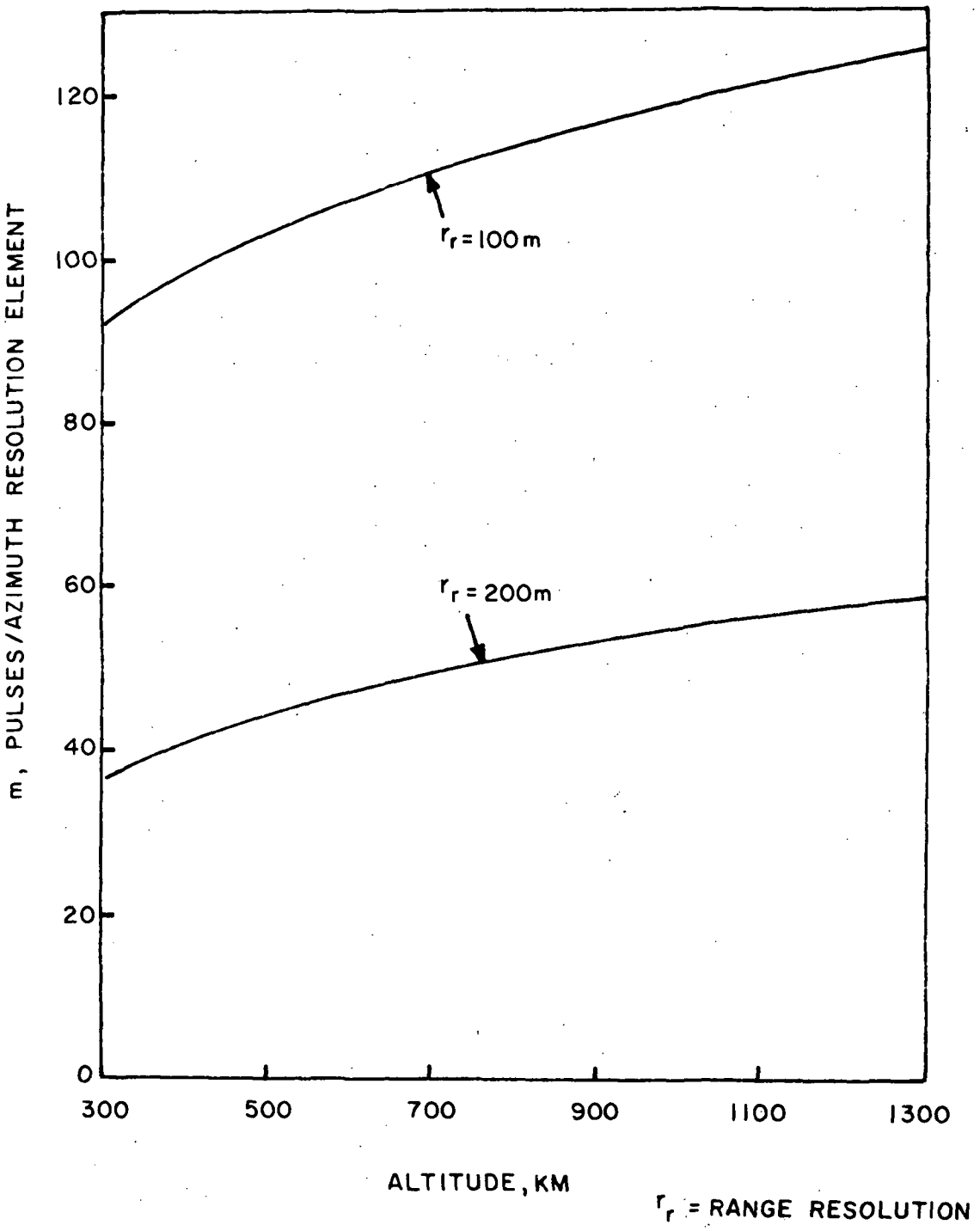

FIGURE 18. MINIMUM NUMBER OF PULSES GENERATED PER AZIMUTH RESOLUTION ELEMENT.

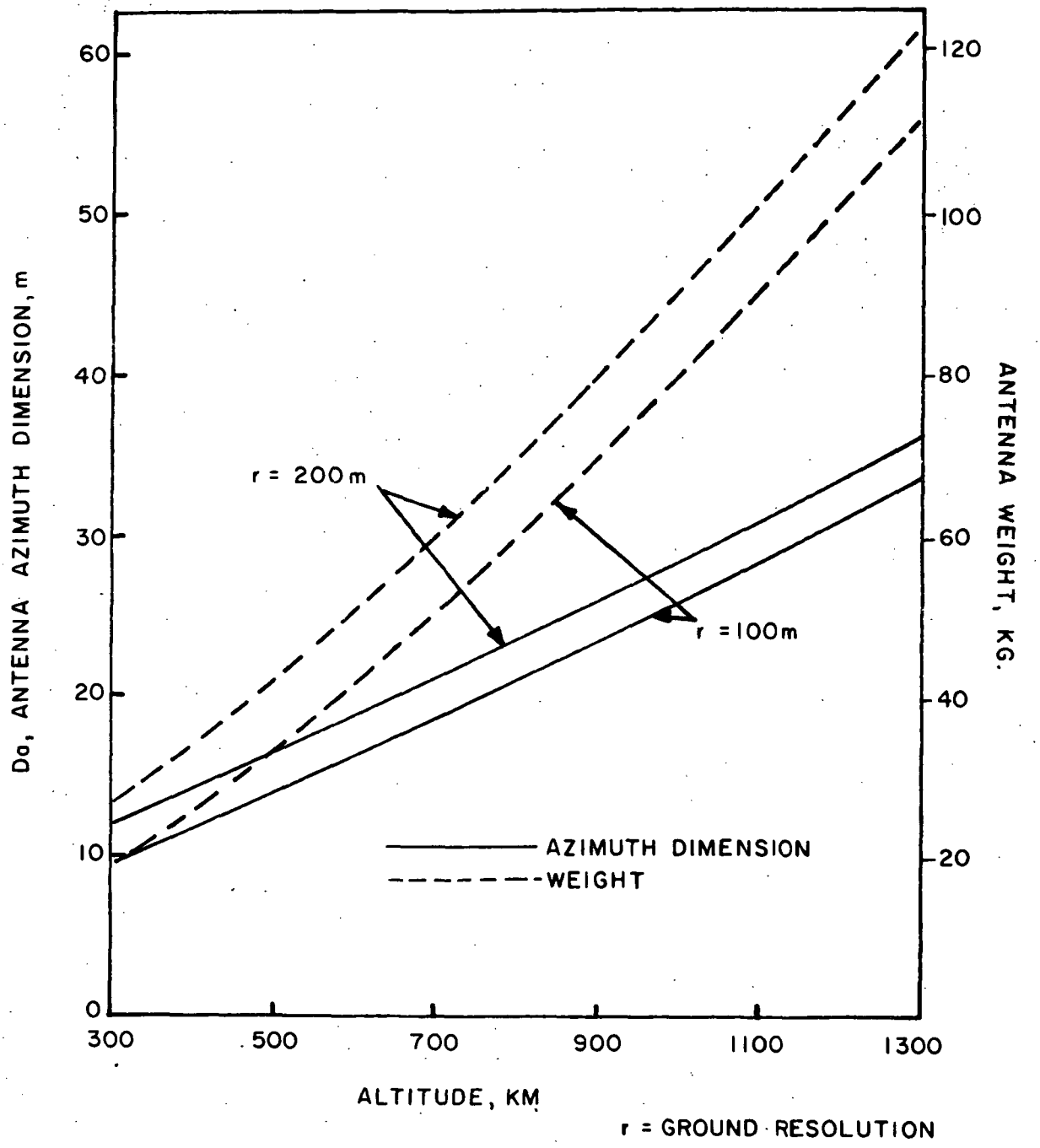

FIGURE 19. ANTENNA SIZE AND WEIGHT VS. ALTITUDE FOCUSED SYNTHETIC APERTURE RADAR (λ = 10cm, α = 45°, Dr = 1.5m)

where the terms have all been previously defined. Just as for the noncoherent system (Section 2.4.1.4),

$$
\begin{aligned}
S/N &= 10 \\
F_o &= 20.24 \\
T &= 700^\circ \text{ K} \\
\beta_r &= 4.75 \\
A &= 1.1 \\
\eta &= 5 \times 10^{-4} \\
\lambda &= 10 \text{ cm}
\end{aligned}
$$

The variation with altitude of required peak powers is shown for 100 and 200 m ground resolution in Figure 20.

The average power is again expressed by

$$\overline{P} = \frac{m \tau P_t}{t_o}$$

where t_o is given by Equation 2.10. The variation in peak power is also shown on Figure 20.

The input power, P_{in}, is dependent on the average power,

$$P_{in} = 100 + 3 \overline{P}$$

The input power, ranging between 120 and 2500 watts, is shown in Figure 21. Notice that these powers are very much higher than those required for noncoherent radar systems at the same altitudes.

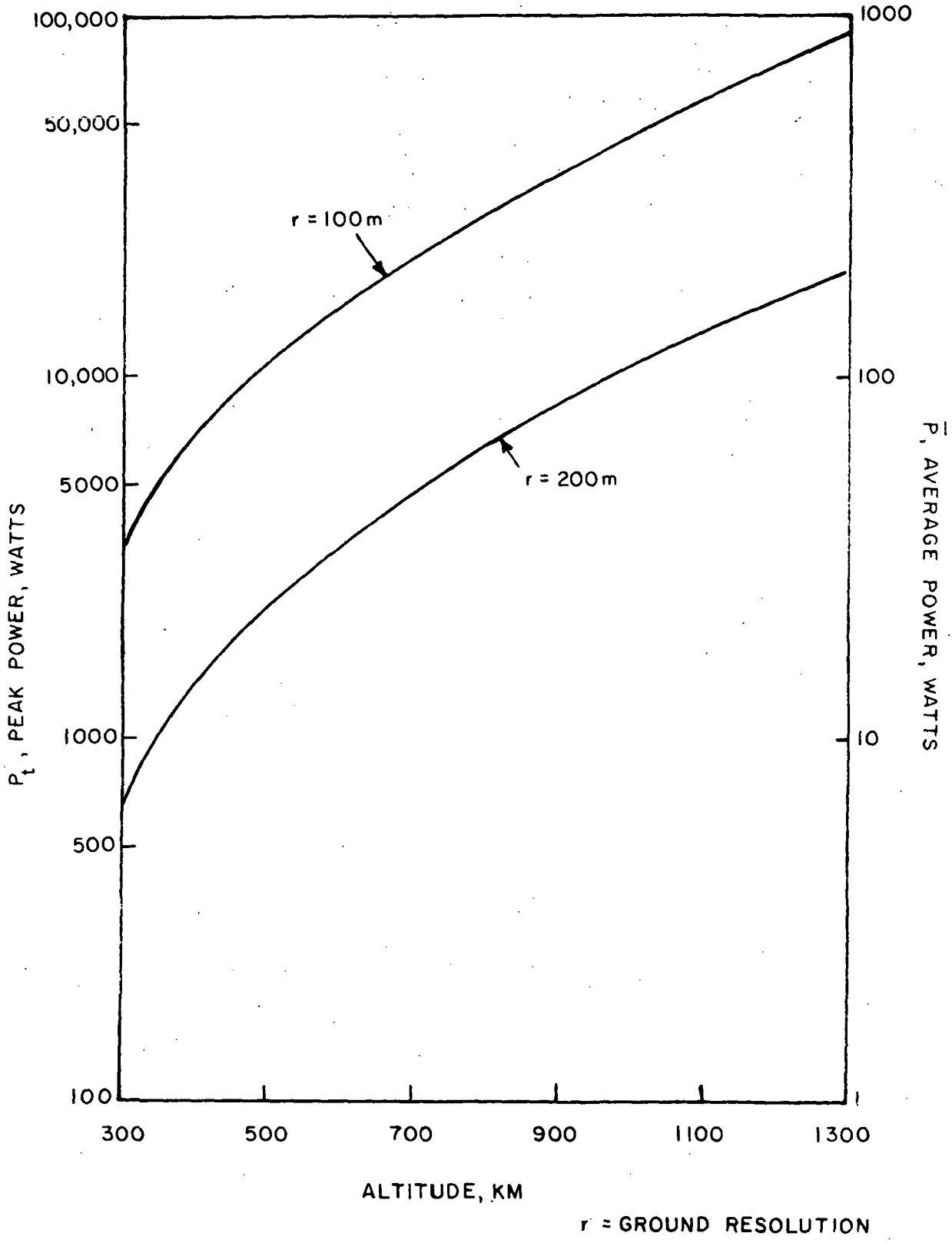

FIGURE 20. PEAK AND AVERAGE POWER VS. ALTITUDE FOCUSED SYNTHETIC APERTURE RADAR.

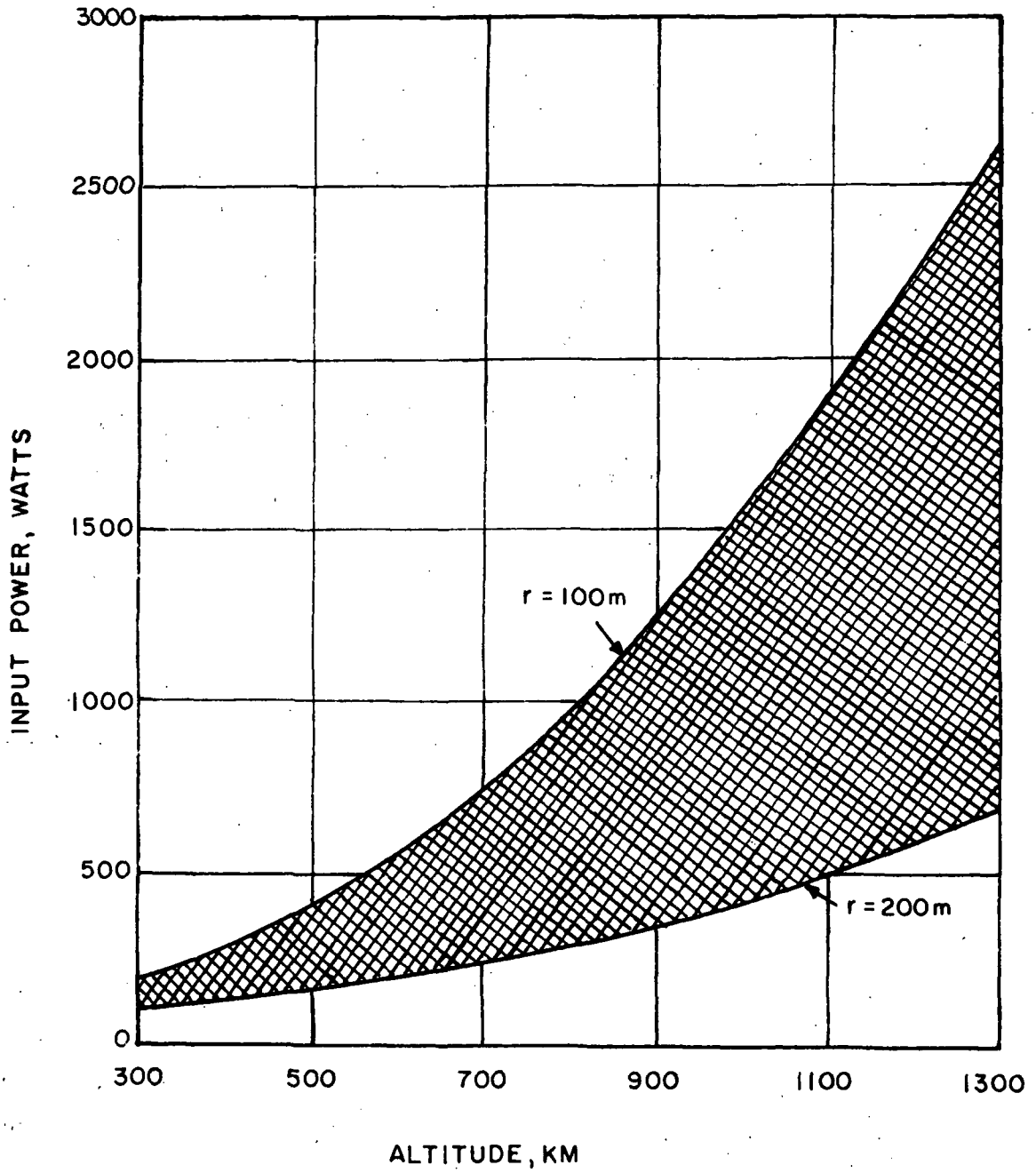

FIGURE 21. INPUT POWER, SYNTHETIC APERTURE RADAR

2.4.2.5 Weight

The weights of the synthetic aperture radar electronics listed in Table 3 are based on the peak power requirements, through the relationship,

$$W_r = 13.6 + 9.1 \ln (0.1 P_t \lambda)$$

The total system weights, the sum of the radar electronics weight and the antenna weight, are shown as a function of altitude in Figure 22. There is very little difference in weight between the high resolution (100 m) and the low resolution systems. The high resolution system requires a higher peak power but a smaller antenna than the lower resolution system. The two requirements just about balance one another in weight, although the higher power system will require a larger spacecraft power supply system.

2.4.2.6 Data Acquisition

The data acquisition rate for synthetic aperture radar systems is obtained by multiplying equation 2.17 by m, the number of pulses;

$$DR \cong \frac{m\,WG}{c\,\tau_c\,t_o} (\cos \Psi_1 + \cos \Psi_2)$$

where G is once again set equal to 6 binary bits per resolution element. The resultant acquisition rate is shown as a function of altitude in Figure 23. The collection rate increases with altitude because of the continuously enlarging swath width, containing resolution elements of a fixed size. This effect is damped slightly due to the decrease in the spacecraft's ground velocity with altitude.

TABLE 3

RADAR ELECTRONICS WEIGHT
SYNTHETIC APERTURE RADAR

Altitude km	Electronics Weight, kg	
	r* = 100 m	r = 200 m
300	45.1	30.5
500	55.5	41.5
700	62.2	48.5
900	67.2	53.7
1100	71.3	58.0
1300	74.8	61.5

* r = Ground Resolution

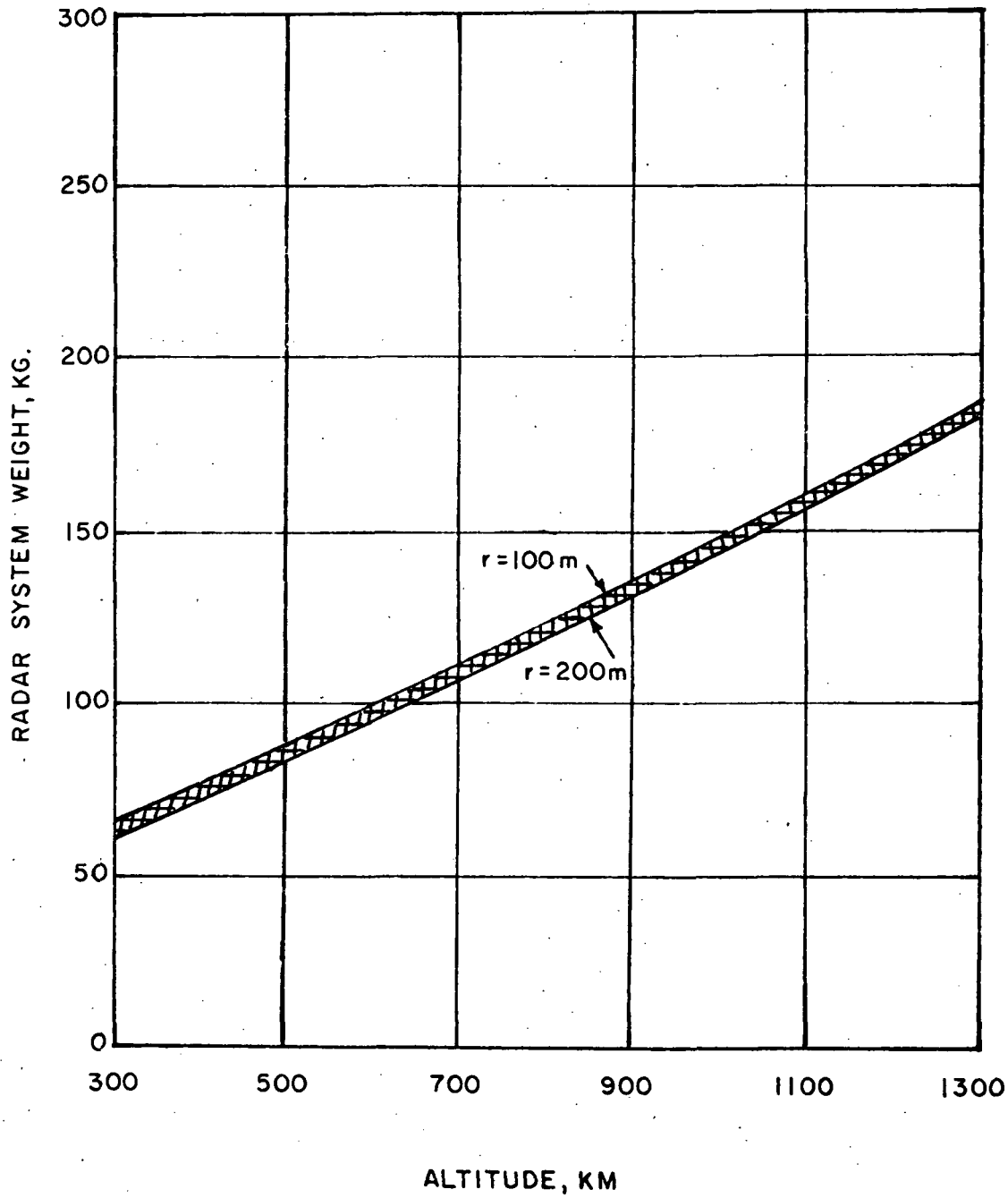

FIGURE 22. TOTAL RADAR SYSTEM WEIGHT (ANTENNA AND ELECTRONICS) FOCUSED SYNTHETIC APERTURE RADAR.

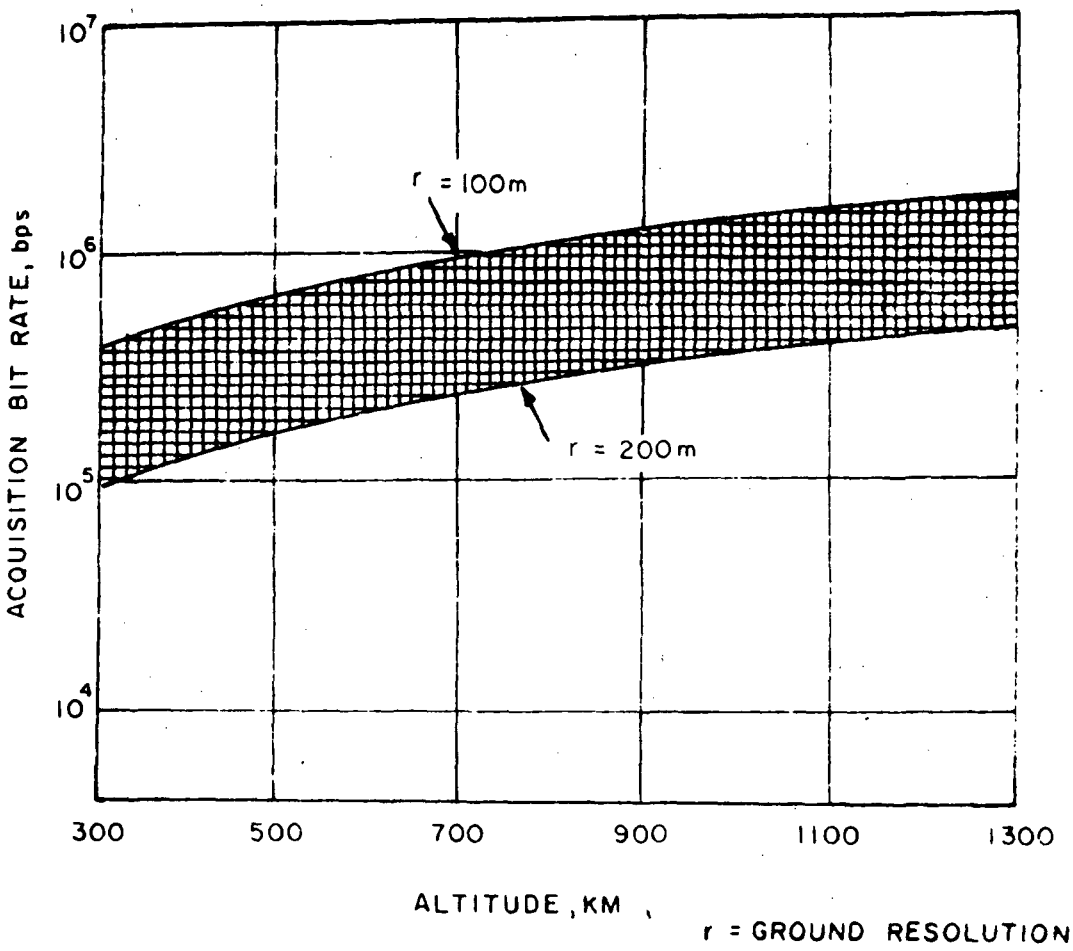

FIGURE 23. ACQUISITION BIT RATE VS. ALTITUDE, FOCUSED SYNTHETIC APERTURE RADAR.

2.4.2.7 Focused Synthetic Aperture Radar Systems - Summary

The focused synthetic aperture radar systems described in this section are able to fully satisfy the requirements for local resolution with antennas under 35 m long and total system weights between 60 and 180 kg. From the viewpoint of these two parameters the synthetic aperture radar is considerably superior to the noncoherent radar discussed previously. However the power requirements and the data acquisition rates are considerably more demanding on the power supply and data handling subsystems than for noncoherent systems. It remains to be seen now how well these two radars fit into a spacecraft. In the next section spacecraft will be sized for each radar over the 1000 km range in altitude, with the effects of their power weight, and data rate requirements on spacecraft subsystems discussed.

3. MISSION ANALYSIS

Now that the radar system requirements have been determined, it remains to size spacecraft to accommodate them. The three spacecraft subsystems most greatly affected by the radar system requirements are the data handling, communications, and power supply. Each of these is also affected by actual orbit parameters such as altitude, inclination, and stay time.

3.1 Orbit Considerations

One of the main problems associated with the low circular orbits (300 km to 1300 km in altitude) used in this study is that of earth and solar occultations. Figure 24 shows typical locations in the orbit (true anomaly) of the earth and solar occultation zones for a 300 km altitude orbit. (For a circular orbit, 0° true anomaly is taken to be the point of injection into the orbit). Even though the figure presents occultation geometry for a Venus mission beginning on a specific arrival date (July 30, 1980), certain observations can be made which apply to all arrival dates considered in this report.

In general, the orbiter will enter zones of earth or sun occultation during almost every orbit and these zones will most frequently overlap. The amount of time in occultation in either zone will be no greater than about forty percent of the orbital period. Although not shown on the figure, Canopus occultation will also occur during every orbit (since a polar orbit at Venus is very nearly polar to the celestial sphere) for about forty percent of the orbital period.

The occultation data presented in Figure 24 is for a "worst case" situation in that the time of occultation per orbit will decrease with increasing orbital altitude. Thus, for an altitude of 1300 km the amount of time in earth or solar occultation reduces to about thirty percent of the orbital period.

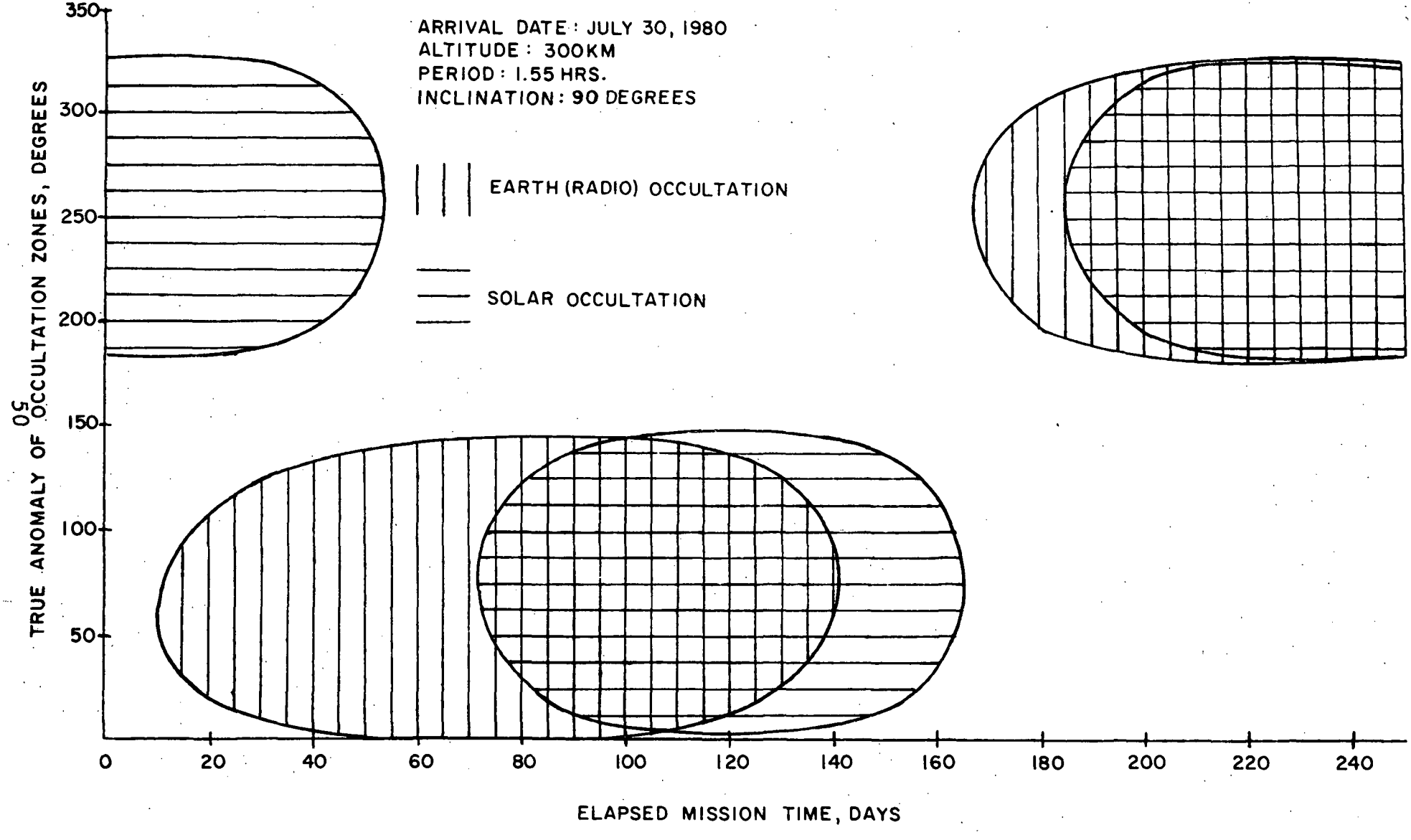

EARTH AND SUN OCCULTATION ZONES FOR MINIMUM ALTITUDE CIRCULAR ORBIT ABOUT VENUS

FIGURE 24.

The polar orbiting spacecraft (in a circular orbit) can completely map Venus' surface in about 120 days. The surface appears to rotate at only ~ 1.5° per 24 hour day under the spacecraft. By mapping a swath between 50 and 250 km in width (and with 20% overlap) the spacecraft must wait between 4 and 18 orbits, depending on altitude, before the next swath comes into view. This time can be used to transmit collected data to earth, and thus lower the load on the communications system considerably. Of course transmission is still possible only outside the earth occultation zones.

The effect of earth and solar occultations on mission operations will depend on the spacecraft's power supply system. In Section 2 it was established that during periods of mapping the radar system would require hundreds of watts (noncoherent radar requires ~ 106 watts and synthetic aperture requires up to 2.5 kilowatts) and acquire large volumes of data, probably more than can be transmitted in real time.

If the spacecraft uses solar cells as the primary power source, there can be no radar mapping during periods of solar occultation, unless the spacecraft carries batteries of sufficient capacity. Also, if the transmission data load is very high, the batteries may be required to provide power to the communication system during solar occultation to maximize available transmission time. Figure 25 illustrates a power profile for a synthetic aperture radar orbiter at 500 km altitude. At this altitude, there are approximately 6.4 orbits from the start of one mapping period to the next. Assuming all mapping is done during one orbit, there are 5.4 orbits available for recharging the batteries and transmitting data. The figure shows a "worst case" situation in that periods of earth and solar occultation do not overlap, possibly requiring the batteries to supply radio power. Note in Figure 25 that the portion of the power profile termed "other" includes general housekeeping and that during periods of mapping and data transmission,"other" also includes the power load for the data handling and storage units.

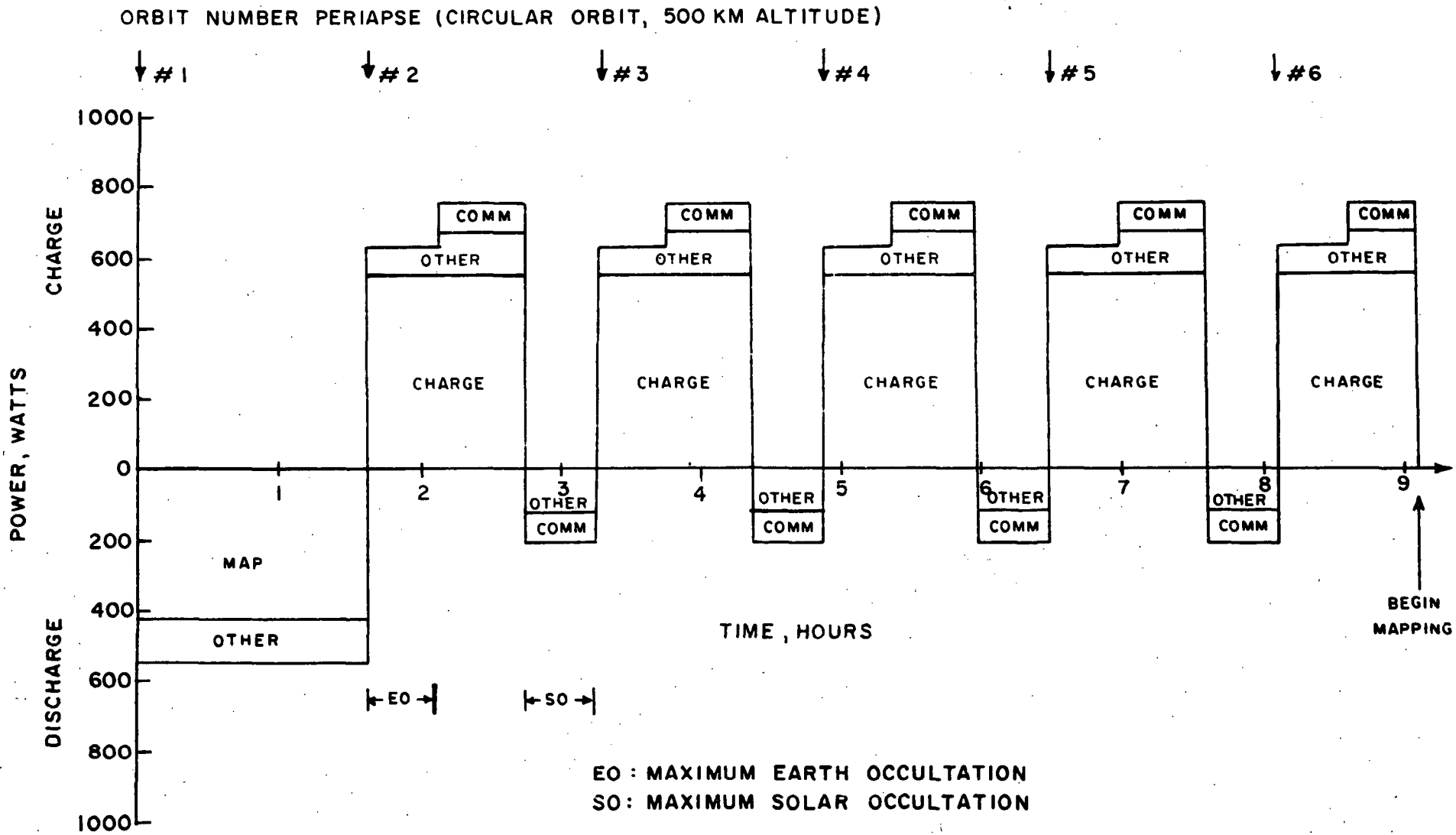

FIGURE 25. REPRESENTATIVE POWER PROFILE BETWEEN CONTIGUOUS MAPPING SWATHS FOR SOLAR CELL/BATTERY POWERED SYNTHETIC APERTURE RADAR SYSTEM.

A spacecraft whose power supply does not depend on the sun (e.g. RTG's) will not have such a complex power profile as one which is solar dependent. Only earth occultations will have an effect on the overall mission operations.

3.2 Minimum Data Transmission Rate

The minimum data transmission rate depends on the data acquisition rate, the number of orbits the system has to telemeter the data collected to earth during the mapping of one swath, and the type of power system. As was seen in Figures 14 and 23 the acquisition bit rate varies from about 10^3 bps for noncoherent to over 10^6 bps for synthetic aperture radar. The minimum rate at which data must be relayed to earth is essentially the total amount of data collected over one orbital pass (the product of the data acquisition rate, the orbital period, and the fraction of the orbit over which mapping occurs) divided by the total amount of time available for transmission before the next swath rotates into view. For a spacecraft which is effectively independent of solar occultations (RTG's or solar cell/battery combination) the radar may map during 100 percent of each orbit and transmit during 60 percent or more of each orbit, depending on altitude and location of the earth occultation zone. Figure 26 illustrates the variation of this data rate with altitude for the synthetic aperture and noncoherent radar systems. Three cases are shown; (1) synthetic aperture with local resolution (100 m $\leq r_r \leq$ 200 m) and 100% coverage of the planet, (2) synthetic aperture with local resolution (100 m $\leq r_r \leq$ 200 m) and 10% coverage, and (3) noncoherent with regional resolution (0.5 km $\leq r_r \leq$ 1.0 km) and 100% coverage. Cases 2 and 3 satisfy the requirement for local and regional coverage, respectively, as discussed in Section 1. Here it was assumed that the spacecraft was earth-occulted for 0.6 hours per orbit, independent of altitude(worse case). The local

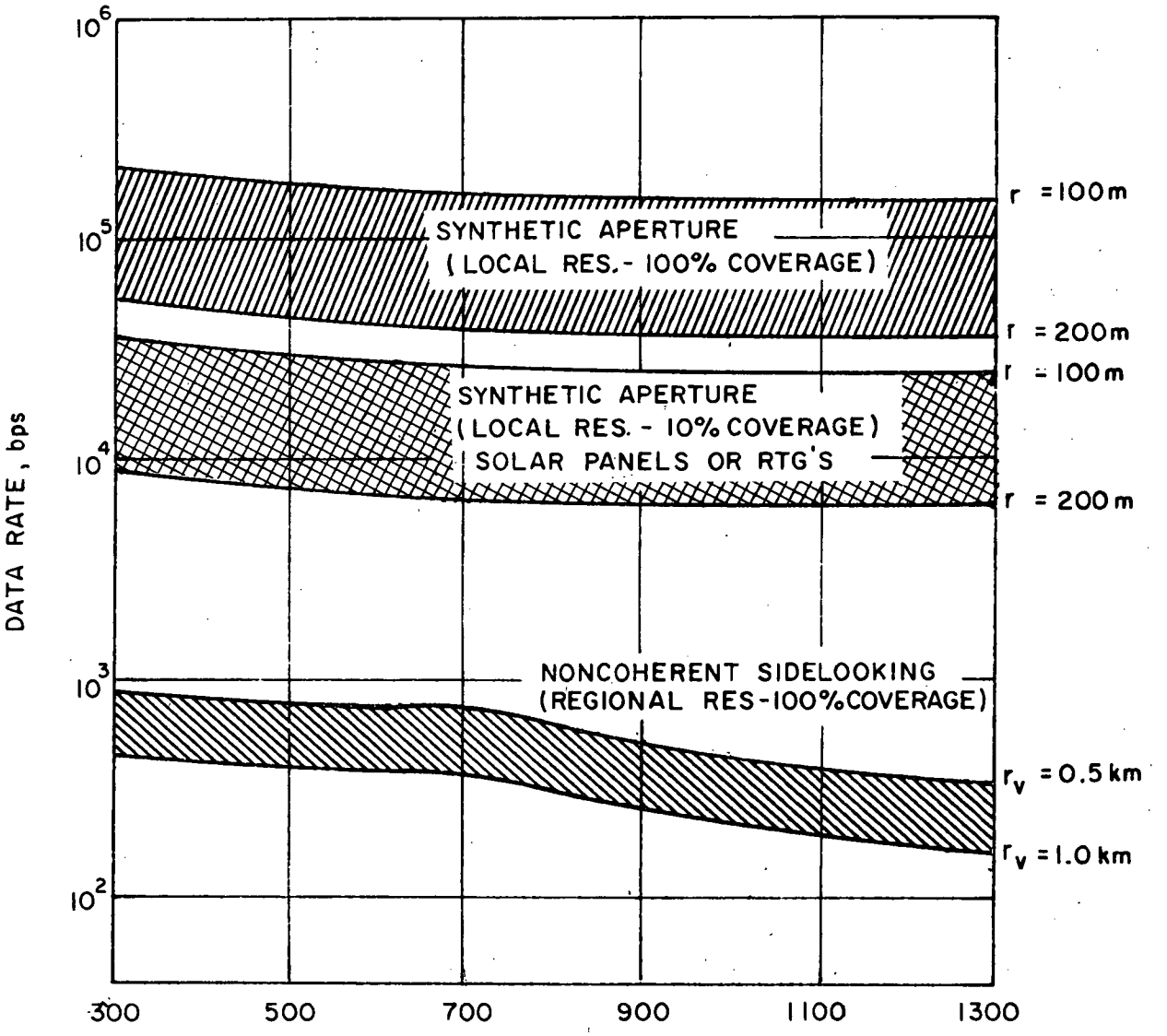

FIGURE 26.

MINIMUM DATA RATE WITH RTG POWER.

coverage is based on mapping for 10 percent of each orbit, again with 0.6 hours earth-occultation factored into the transmission time. Case 1 illustrates the resulting increase (10X) in data load if the entire surface were to be mapped at 100-200m resolution.

If the spacecraft's power supply is from solar cells alone, i.e., without sufficient battery capacity to power the radar system during solar occultations, only 70-80 percent of Venus' surface can be mapped. The average data rate over the whole 120 day mission will be proportionately lower. The actual minimum permissable data rate, however, will depend on the placement of the earth and solar occultation zones.

The spacecraft's communication subsystem was sized to provide a data transmission rate between the minimum, shown on Figure 26, and the maximum, the data acquisition rate given in Figures 14 and 23. After reviewing the advantages of the synthetic aperture system it was decided to size its data storage capacity to handle the data accumulated in the mapping of 100 percent of Venus' surface, rather than the 10 percent called for in Section 1. This provides excellent resolution of the entire surface for, as will be seen, very little penalty in weight and power.

3.3 Spacecraft Sizing

The primary consideration in sizing a spacecraft for the radar mapping of Venus was the power supply subsystem. As was indicated previously, a spacecraft using RTG's is somewhat more flexible when considering the mission's sequence of events in orbit (i.e., mapping and transmitting data). A further consideration in favor or RTG's is that of attitude pointing. During periods of mapping, the radar antenna must be kept pointed at the correct area on the surface with a high degree of accuracy. If the spacecraft uses solar cell power alone,

then the solar panels must be kept normal, or very nearly normal to the spacecraft - Sun line for maximum efficiency. This double pointing requirement would lead to severe mechanical requirements throughout a single orbit. The problem is further complicated by the fact that the orbit is inertial in space, so that the apparent position of the sun will move through about 180° in the Venus orbit plane during 120 days of elaped mission time. Thus the solar panel pointing mechanism must also account for the Sun's apparent motion about the orbit plane. If the spacecraft uses a solar cell/battery combination power supply, the problem shifts to one of rotating the spacecraft back and forth between the proper attitudes for mapping, charging the batteries, and transmitting data. The possibility of a dual pointing requirement exists if the spacecraft must charge and transmit simultaneously in order to maximize transmission time.

The use of RTG's eliminates the triple pointing problem. During mapping, the only pointing constraint is that of the radar antenna to the surface, and during transmission of radar data, the constraint is that of the high gain antenna to the earth.

RTG's were used as the spacecraft power supply except for those cases for which the radar system required more than 750 watts of input power (see Figure 21). The RTG's assumed for sizing purposes are those currently being developed for the TOPS (Grand Tour), each RTG weighing 29.5 kg and supplying 140 watts of raw power. The scope of this study did not permit a detailed investigation of the thermal and nuclear radiation properties of RTG's in the Venus environment. It is noted that this may present a serious problem and should be studied in detail.

It appears that the most practical source of power for those radar systems requiring about one kilowatt would be solar cells since the weight penalty for sufficient RTG's

would become prohibitive. The power levels for these radar systems approach the power levels of small solar electric propulsion stages. It is possible, then, to utilize the solar panels from the SEP as the power supply for the radar system and design on integrated SEP/spacecraft. This approach was considered in this study. High power cases were constrained to the use of solar electric low-thrust Earth-Venus transfers. The spacecraft subsystems were sized as being integrated with the SEP module.

Table 4 lists spacecraft subsystem weights for selected examples of radar system, altitude and resolution. The first example depicts a spacecraft with a noncoherent radar at 500 km altitude and a vertical resolution of 0.5 km. The radar system requires 101 watts of power and RTG's are used as the power supply. The second example shows a spacecraft with synthetic aperture radar at 500 km altitude and a range resolution of 100 m. The radar requires 424 watts of power and again RTG's are used for power. For comparison, the third example shows the same radar system and altitude, but uses solar cell/battery combination for power supply. As may be expected, the use of RTG's leads to an overall heavier spacecraft for the same power output as one which uses solar panels and batteries. In the final example, a synthetic aperture radar orbiter at 1100 km and 100 m range resolution, the radar system requires over 1800 watts of power, thus an integrated SEP/spacecraft is assumed. The weight budget for solar panels is not shown since it would be scaled primarily for the SEP and would therefore appear in the SEP subsystems weight allocation. Note, however, that power conditioning equipment and a small battery for housekeeping are included in the spacecraft module.

The solar panels, batteries and power conditioning equipment in the power subsystem, the control computer and sequencer, attitude control, cabling, thermal control and structure and mechanical devices were sized by use of scaling laws developed by Dunkin and Spadoni (1972). As mentioned

TABLE 4

SPACECRAFT SUBSYSTEMS NOMINAL WEIGHT ALLOCATIONS

RADAR SYSTEM	NONCOHERENT	SYNTHETIC APERTURE		
ORBIT ALTITUDE/RESOLUTION	500 km/r_v=0.5 km	500 km/r=100 m	500 km/r=100 m	1100 km/r=100m
SPACECRAFT CLASS	ADVANCED MARINER	VIKING/TOPS	VIKING/TOPS	INTEGRATED SEP
PRIMARY POWER	RTG'S	RTG'S	SOLAR CELL/ BATTERY	SOLAR CELLS
SUBSYSTEM WT. BREAKDOWN				
Radar	152 kg	89 kg	89 kg	161 kg
Power	123[a]	193[b]	73[c]	17[d]
Data Handling & Storage	20	56	56	42
Control Computer & Sequencer	14	14	14	14
Attitude Control	77	77	77	77
Telecommunications	39	66	66	66
Cabling	22	29	32	34
Thermal Control	13	17	19	20
Structure & Mechanical Devices	131	134	122	140
Contingency	59	67	55	57
TOTAL	650	742	604	628

a) Includes three 140 watt RTG's

b) Includes five 140 watt RTG's

c) Includes battery and fold-out solar panels

d) Battery and conditioning equipment only.

previously, the RTG's proposed for TOPS were assumed for those systems using RTG's. An overall subsystems contingency factor of 10% was assumed.

Data handling and storage, and telecommunications subsystems were sized from proposed hardware designs of Mariner (1973) and TOPS Technology. The Mariner subsystems were used for the noncoherent radar, having low data acquisition and transmission rates. A 20-watt TWTA S-band transmitter and 40 inch high gain antenna yield a maximum transmitted bit rate (16.2 kbps) which is well above the requirements for noncoherent radar. The Mariner magnetic tape recorder has a storage capacity (1.8×10^8 bits), adequate for the noncoherent radar system.

Since data transmission and storage requirements for synthetic aperture radar are much greater than those for noncoherent radar, more sophisticated electronics than the Mariner technology level are required. The 40 watt S- and X-band TWTA transmitter from TOPS using a 9 foot rigid paraboloid high gain antenna can provide a transmitted bit rate of 1.8×10^5 bps for low altitude synthetic aperture radar. Mass data storage for synthetic aperture is on the order of several billion bits. The proposed tape recorders for TOPS have a capacity of 10^9 bits each; thus, multiple units of TOPS tape recorders were used as required by the synthetic aperture system.

All of this is not to say that these electronic subsystems can be utilized in a high data rate radar orbiter without modification. They were selected to indicate weight allowances typical of anticipated hardware designs. New technology requirements for these subsystems should not be any more significant than those required for the radar system itself.

Figure 27 presents spacecraft weight in orbit for the radar systems, resolutions and range of orbit altitudes considered in this study. The curves are for RTG powered spacecraft, except where noted, since this will yield the heaviest spacecraft concept and thus indicate an upper limit to the required payload curves.

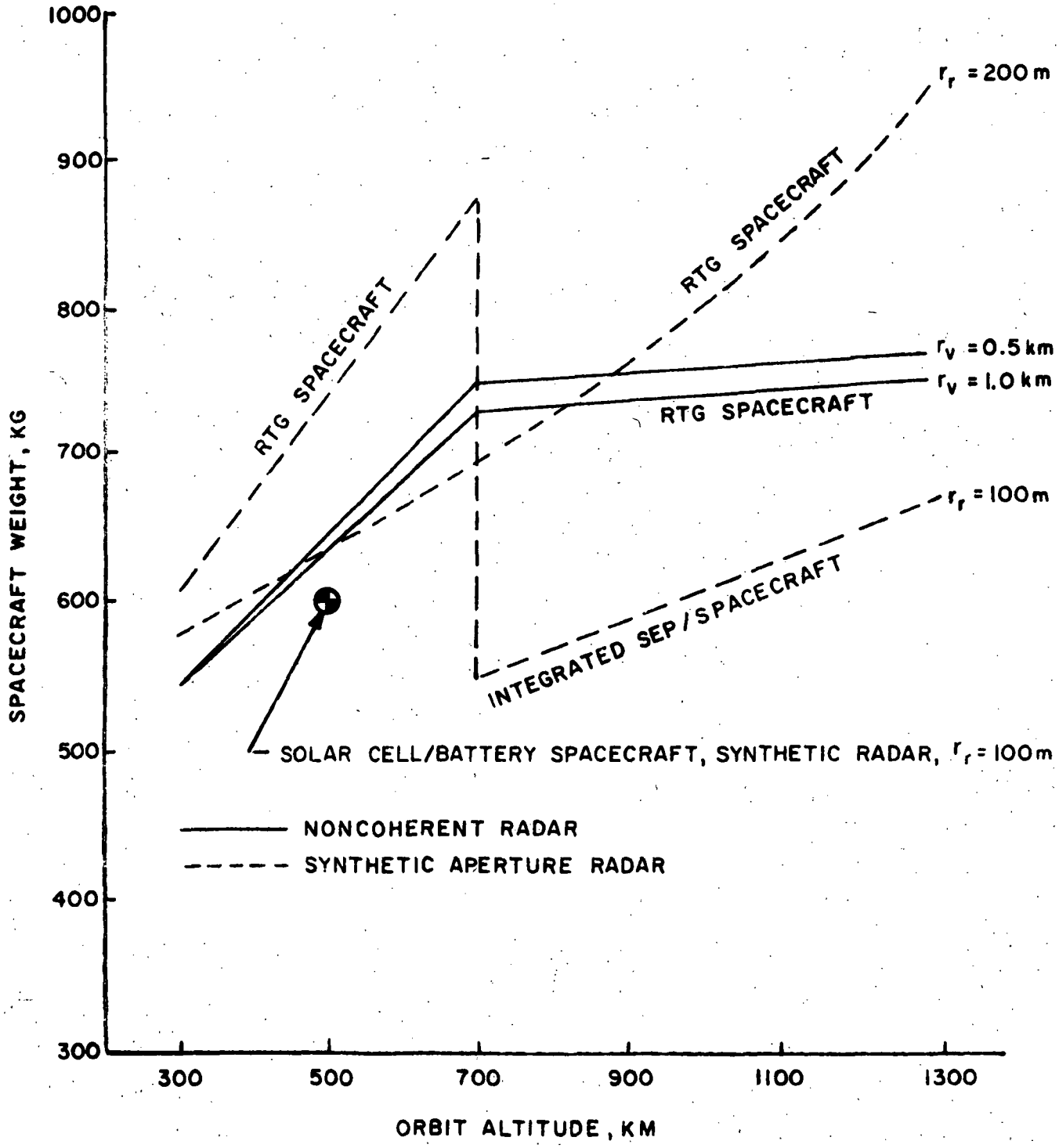

VENUS RADAR MAPPING SPACECRAFT, REQUIRED WEIGHT IN ORBIT.

FIGURE 27.

High resolution synthetic aperture systems require over 750 watts of power at altitudes over approximately 700 km, hence the curve switches to an integrated SEP/spacecraft concept. The weight of the SEP module is not included in this portion of the curve. The point labeled "solar cell/battery spacecraft" corresponds to the third example in Table 4, and is shown on Figure 27 for comparison.

3.4 Trajectory and Payload Analysis

Table 5 presents the Earth-Venus interplanetary transfer data which were used for determining launch vehicle payload capability. Earth-Venus ballistic trajectory data from 1978 to 1985 were searched for the launch time which yielded the lowest combination of departure and arrival velocities (i.e., minimum total energy) for each launch opportunity. The effects of launch window constraints were not included. Note that the late 1984 opportunity is the only one that approaches the launch constraint of $\pm$ 36° declination at ETR.

The best available SEP data (Horsewood and Mann, 1970) were used to find suitable Earth-Venus SEP transfers as an alternative spacecraft delivery system. The data is two-dimensional, thus no information is available as to specific launch dates or launch and arrival geometries. The data is merely representative of SEP capability. The data is presented in a form which is launch vehicle dependent. SEP transfers were chosen which yielded adequate final mass at a minimum power level. The Titan IIIC(7) data was scaled from Titan IIIC data by scaling methods developed by Bartz and Friedlander (1971). Note that the selected power levels of the SEP stages are more than adequate for use as power supply systems for the high altitude, high resolution synthetic aperture radar systems.

TABLE 5

EARTH-VENUS TRAJECTORY DATA

BALLISTIC:

Launch Date	Flight Time (Days)	C_3 (km^2/sec^2)	DLA (DEG)	VHP (km/sec)
8/20/78	120	9.060	8.7	5.126
4/11/80	110	15.705	- 9.9	4.530
12/2/81	110	18.931	3.7	2.920
6/5/83	150	7.193	-11.7	3.040
12/6/84	170	13.653	32.1	2.771

SOLAR ELECTRIC* (LAUNCH VEHICLE DEPENDENT):

Launch Vehicle	Flight Time (Days)	C_3 (km^2/sec^2)	P_o (1 au) (kwe)	m_f/m_o	VHP (km/sec)
Titan III C (7)	140	5.308	3.3	0.950	2.493
Titan III D/Centaur	150	5.130	3.7	0.983	2.461

* Two-dimensional low thrust analysis (Horsewood and Mann 1970)

Figure 28 presents the payload capability of the Titan IIID/Centaur launch vehicle for the ballistic interplanetary transfers. The propulsion system assumed for orbit capture is a pressure-fed Earth-storable system having a 295 sec Isp. Comparing Figure 27 with Figure 28, only the 1983 opportunity provides sufficient payload capability for both radar systems and all orbit altitudes under consideration. The 1981 and 1984 opportunities do provide sufficient payload capability with the Titan IIID/Centaur, at lower altitudes (see Figure 27), whereas the 1978 and 1980 opportunities are inadequate with this launch vehicle. Should greater payload capability be required, either a larger launch vehicle, such as the Titan IIID(7)/Centaur, an orbit insertion propulsion system with a higher mass fraction (e.g. space-storable propellant) can be utilized or elliptical orbits would have to be considered.

Figure 29 presents the payload capability of the SEP systems given consideration. The weight of the SEP stage is not included in the non-jettisoned payload curves. The Titan IIID/Centaur with a 3.7 kw stage provides more than adequate payload capability, even though the SEP stage is carried into orbit with the spacecraft, whether or not it is utilized in an integrated concept. It can, of course, be jettisoned prior to orbit insertion, thus providing even greater payload capability.

The Titan IIIC(7) launch vehicle with SEP does not provide adequate payload capability over the full range of radar systems and orbit altitudes considered. Comparing Figures 27 and 29, it can be seen that (excluding the integrated SEP/spacecraft curve) the non-jettisoned curve provides only marginal payload capability at the lowest altitude, and the jettisoned payload curve is only somewhat more adequate. Note, though, that the non-jettisoned payload curve for the Titan IIIC(7) does provide sufficient payload capability for those radar systems which could utilize the integrated SEP/spacecraft concept.

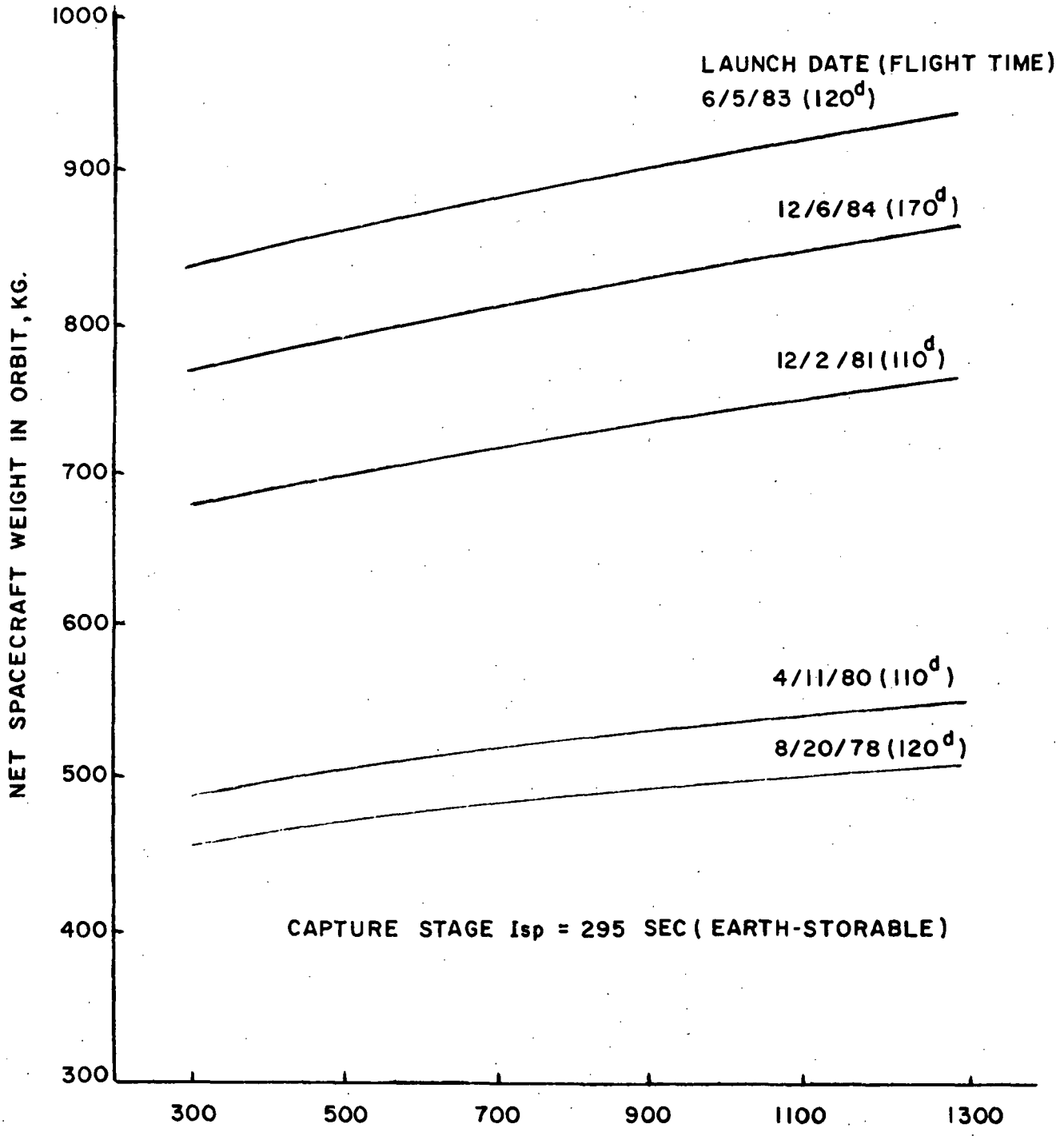

FIGURE 28.

VENUS RADAR IMAGING ORBITER TITAN IIID/CENTAUR BALLISTIC PERFORMANCE.

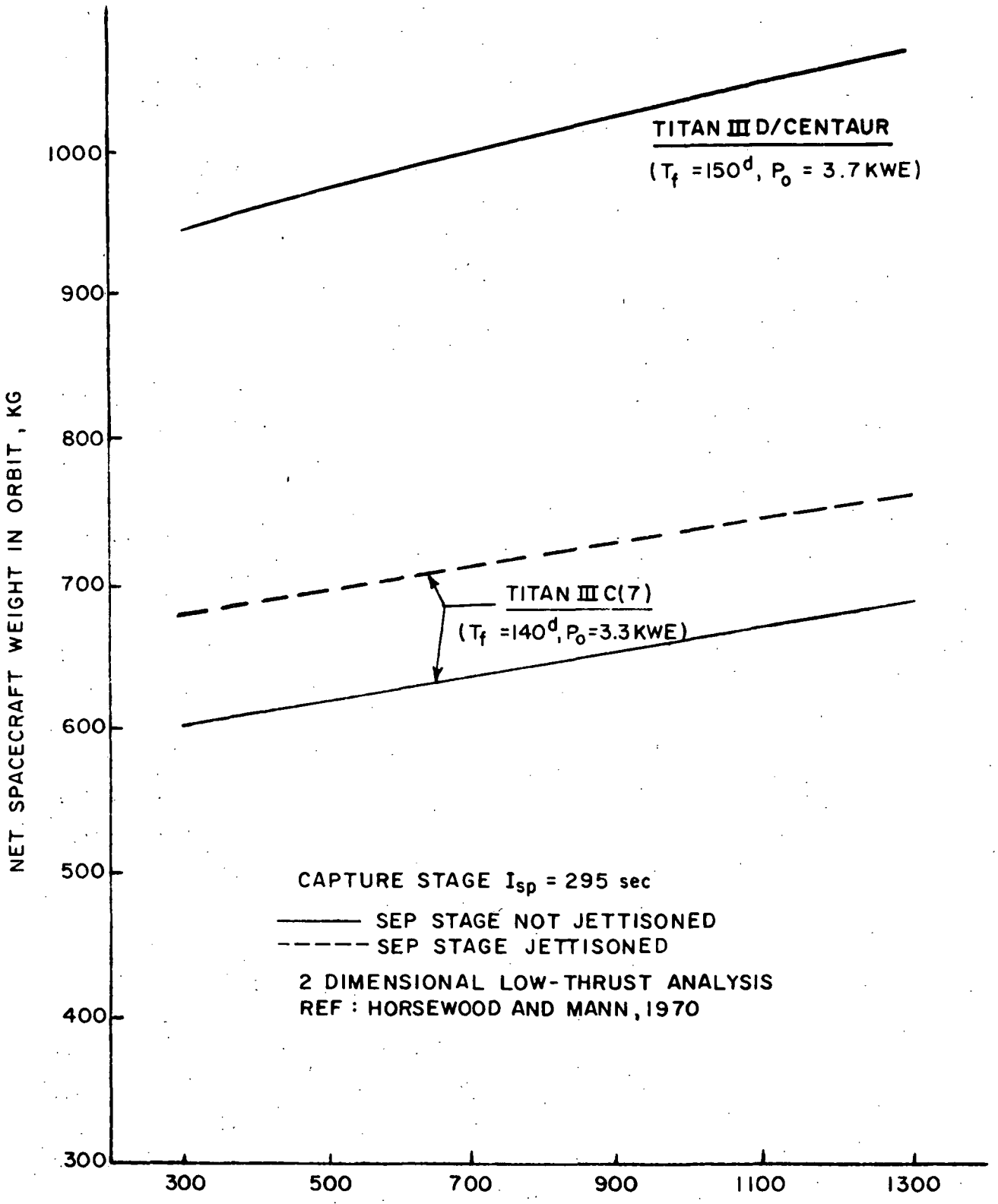

FIGURE 29.

VENUS RADAR IMAGING ORBITER, SOLAR ELECTRIC PROPULSION CAPABILITY

3.5 Sample Missions

Comparing the spacecraft weight curves (Figure 27) with the launch vehicle capability curves (Figures 28 and 29) it is evident that there are a large number of mission combinations possible. There are four possible combinations of delivery mode and radar system; ballistic with noncoherent or synthetic aperture radar, and solar electric propulsion with noncoherent or synthetic aperture radar. Table 6 contains the spacecraft subsystem breakdown for a sample mission of each combination. For each sample a low altitude orbit was chosen to keep the antenna size down, and to reduce the pointing problems, required power and system weight.

Sample mission I is a ballistically delivered non-coherent radar system in a 300 km orbit. The radar system consists of a relatively small (for non-coherent) antenna with 14 kg of electronics and is able to provide 0.5 x 3 km spatial and 0.5 km vertical resolution of the entire planetary surface in 58.5 km swaths. Three 140 watt RTG's are required for the spacecrafts operation, including 101 watts of radar input power. The Mariner '73 communications and data handling and storage subsystems are adequate for this mission even though the spacecraft may be earth-occulted for a fairly large fraction of each orbit. The total spacecraft mass is 545 kg. and, referring back to Figure 28, can be launched with the Titan IIID/Centaur in '81, '83 or '84, with the 12/2/81 launch providing the shortest (110^d) flight time.

Sample mission II illustrates the ballistically delivered synthetic aperture system. The 90 kg. radar system consists of a 34 kg., 1.48 x 14.3 m antenna and 56 kg. of electronics, and is capable of 100 percent surface coverage at 100 x 100 m spatial and 100 m vertical resolution. Five RTG's are necessary for spacecraft power supply due to the 424 watt radar power requirement. The more advanced TOPS communication

TABLE 6 FOUR SAMPLE VENUS RADAR MAPPING MISSIONS

	I	II	III	IV
DELIVERY MODE RADAR SYSTEM	BALLISTIC NONCOHERENT	BALLISTIC SYNTHETIC APERTURE	SEP NONCOHERENT	SEP SYNTHETIC APERTURE
ALTITUDE ORBIT PERIOD	300 km 1.57h	500 km 1.64h	500 1.64h	700 km 1.72h
RESOLUTION AZIMUTH RANGE VERTICAL SWATH WIDTH	 3.0 km 0.5 km 0.5 km 58.5 km	 100 m 100 m 100 m 87 km	 3.0 km 0.5 m 0.5 m 98 km	 100 m 100 m 94 m 129 km
LAUNCH VEHICLE LAUNCH DATE	TIIID/C '81,'83, '84	TIIID/C '83,'84	TIIIC(7)- JETT SEP -	TIIIC(7)-INT SEP/ SPACECRAFT -
SPACECRAFT POWER SYSTEM COMMUNICATIONS DATA STORAGE	545 Kg 3RTGs* 20 WATT TWT, 40" ANT., SBAND 46 Kg $1.8x10^8$ bits 9 Kg	741 Kg 5RTGs* 40 WATT TWT, 9' ANT., XBAND 61 Kg $4x10^9$ bits 56 Kg	650 Kg 3RTGs* 20 WATT TWT, 40" Ant., SBAND 46 Kg $1.8x10^8$ 9 Kg	550 Kg + SEP SEP POWER SUPPLY 40 WATT TWT, 9' ANT., XBAND 61 Kg $2x10^9$ bits 42 Kg
RADAR SYSTEM WAVELENGTH DEPRESSION ANGLE ANTENNA WEIGHT PEAK POWER INPUT POWER PULSE WIDTH PRF ELECTRONICS WEIGHT	73 Kg 10 Cm 45° 1.5x21.5 m 59 Kg 93 WATTS 101 WATTS $4x10^{-4}$ SEC 3 pps 14 Kg	90 Kg 10 Cm 45° 1.48x14.3 m 34 Kg 10^4 WATTS 424 WATTS $9.4x10^{-5}$ SEC 1800 pps 56 Kg	152 Kg 10 Cm 45° 1.5x37.0 m 131 Kg 222 WATTS 101 WATTS $4.6x10^{-4}$ SEC 2.4 pps 21 Kg	112 Kg 10 Cm 45° 1.48x19.0 m 50 Kg $2.1x10^4$ WATTS 769 WATTS $9.8x10^{-5}$ SEC 1306 pps 62 Kg
DATA RATE MAX ACQ. MIN TELE. (AT 10% COVERAGE)	 2000 bps 880 bps	 $6.25x10^5$ bps $1.8x10^5$ bps ($3x10^4$ bps)	 3100 bps 760 bps	 $8.8x10^5$ bps $1.08x10^5$ bps ($2.8x10^4$ bps)

*1 RTG = 140 WATTS

and data handling subsystems must be used together with 4 10^9 bit capacity tape transports to handle the high resolution data load. Referring again to Figure 28, the 741 kg. spacecraft can be delivered to the 500 km circular Venus orbit by the Titan IIID/Centaur in '83 or '84, with the 6/5/83 launch providing the s shortest flight time (120^d) and the largest payload margin.

An SEP delivered, noncoherent radar orbiter is illustrated by Sample III. Again in a 500 km polar circular orbit this radar system is designed to provide 0.5 x 3 km spatial and 0.5 km vertical resolution of 100 percent of Venus' surface. At this altitude a 1.5 x 37 m antenna weighing 131 kg. is required. The radar electronics, requiring 101 watts of input power, weight only 21 kg. The Mariner '73 communications and data handling and storage systems are adequate for this mission as in Sample I. The 650 kg. spacecraft can be delivered using a 3.3 KWE SEP stage on a Titan IIIC(7) Centaur (see Figure 29) in 140 days, if the SEP stage is jettisoned before orbit insertion. Since the low (101 watt) radar power requirement may easily be supplied by 3 RTG's, jettisoning the SEP stage is not a mission drawback. It is, rather, an advantage as the problems involved in solar-panel pointing may be ignored.

Sample Mission IV is an example of a SEP delivered synthetic aperture radar system. The 112 kg. radar consists of a 1.48 x 19 m, 50 kg. antenna and 62 kg. of electronics, and provides 100 x 100 m spatial and 94 m vertical resolution of at least 75 percent of the planets surface. Because of the large amount of data collected in one orbital pass the TOPS communication and data handling and storage system must be used, as it was for Sample II. The high (769 watts) radar power requirement necessitates the use of a solar cell power supply system. The integrated SEP stage-spacecraft concept was therefore chosen for this example. Figure 29 shows that the 550 kg. spacecraft (less SEP stage) can be delivered by the Titan IIIC(7) launch vehicle with a flight time of 140 days. Some surface coverage is lost

due periods of solar occultation when enough power for mapping is not available. This may be, however, overcome by the addition of batteries. The added constraint of solar panel pointing must also be considered as a drawback of this mission.

It is interesting to note from Table 6 that while the noncoherent radar produces spatial resolutions over thirty times worse than the synthetic aperture system, the total spacecraft weights are nearly equal. Thus with the wide launch vehicle capabilities previously illustrated there is a definite tendency to favor the synthetic aperture system for mapping where the differences in weight between the two systems are minimal, and if data handling for synthetic aperture radar presents no problems.

4. CONCLUSIONS AND RECOMMENDATIONS

This study has demonstrated in a preliminary manner the feasibility of using both noncoherent side-looking and focused synthetic aperture radar systems to map the surface of Venus from an orbiting spacecraft. Of course since this study is preliminary it has overlooked many of the systems-oriented problems, but it has shown that the major system's requirements are within the realm of current technology.

The spacecraft masses for both radars, sized by a fairly conservative method, fall within the 500 to 1000 kg. range. These masses are well within the capabilities of the Titan IIID/Centaur, using either the ballistic or SEP delivery modes.

The fabrication, storage, and deployment of the long (20-50 m) radar antennas required by the non-coherent system may be a problem. The synthetic aperture system requires antennas about half as long as the non-coherent, and this may be reduced by increasing the peak power and pulse repetition frequency. Further work in the design of long rectangular antennas needs to be done before the problem can be better assessed.

The power requirements of the two radars range from 100 watts to 2.5 kilowatts, and are not beyond the capacities of current power systems. Operations at Venus make the RTG-type power unit preferable to solar panels because of the former's independence of the sun's position relative to the spacecraft. The RTG's eliminate the need to have the spacecraft maintain orientations in three directions; toward the sun for the solar panels, toward the earth for communications and precisely toward the planet's surface for the radar, and thus relaxes the constraints on the attitude control system. The thermal output of the RTG's and its effects on the spacecrafts design was not investigated in this study. It could be that this is a disadvantage which negates the RTG's advantages.

Current data and communications systems are adequate for use with the noncoherent system, but may be only marginal for the synthetic aperture system. The latter requires a data storage system able to accept data at over one megabit a second (for the high altitude cases), very near the current system limits. Also, the communications requirements are very close to the DSN ground transmission limit (1-2.5 x 10^5 bps).

This study has demonstrated the superiority of the synthetic aperture system over the noncoherent. Although the noncoherent radar is a less sophisticated system requiring a low input power, its total spacecraft weight is about equal to that of the synthetic aperture radar system. This is due chiefly to the large antenna required by the noncoherent system, and with a limit of about 50 meters on antenna size there is no way in which resolution better than one kilometer can be obtained. Synthetic aperture radar, on the other hand, has a large growth potential. Its resolution capabilities are not so closely tied to antenna size as the noncoherent radar, which allows for much more flexibility of design. Furthermore, advancements in radar and spacecraft technology should continue to improve the overall feasibility of the synthetic aperture radar system for space missions. In view of the fact that earth-based radar observations of Venus are approaching the capability of a noncoherent system, it would seem most reasonable to emphasize development of synthetic aperture radar for a comprehensive Venus mapping mission in the early 1980's.

BIBLIOGRAPHY

Bartz, D. R. and Friedlander, A. L., "Performance Scaling Laws for Electric Propulsion Mission Analysis", AIAA Paper No. 71-160 Jan. 1971.

Battan, L. J., Radar Meteorology, University of Chicago Press, 1959.

Brindley, A. E., Private Communication (Electronics, IITRI).

Couvillon, L. A., "Communicating with Outer-Planet Spacecraft", Astronautics & Aeronautics, Vol. 8, No. 9, September 1970.

Dunbar, C. O. and Rodgers, J., Principles of Stratigraphy, John Wiley and Sons, Inc. 1957.

Eckman, P. K., et al., "Mariner Venus/Mercury 1973 Study", Technical Memorandum 33-434, Jet Propulsion Laboratory, August 1969.

Evans, J. V. and Hagfors, T., Radar Astronomy, McGraw-Hill, 1968.

Fleagle, R. G., and Businger, J. A., Atmospheric Physics, Academic Press, 1963.

Goldman, H., and Brandenburg, R. K., "Potentials of Spacecraft Radar", IITRI/Astro Sciences Report No. 58 August 1971.

Greenberg, J. S., "A Systems Look at Satellite-Borne High Resolution Radar", RCA Review, December 1967, pp. 679-709.

Heer, E., and Yang, J. N., "Optimization of Space Antenna Structures", JPL Technical Memorandum 33-472, April 1, 1971.

Horsewood, J. L. and Mann, F. I., "Optimum Solar Electric Interplanetary Trajectory and Performance Data", NASA CR-1524, April 1, 1970.

Klopp, D. A., (ed) Orbital Imagery for Planetary Exploration, Vol. III, Definitions of Scientific Objectives, IITRI/Astro Sciences, August 1969.

Klopp, D. A., Orbital Imagery for Planetary Exploration, Vol. IV, Imaging Sensor System Scaling Laws, IITRI/Astro Sciences, September 1969.

BIBLIOGRAPHY (continued)

Martin, B. D., "Data Subsystems for 12-Year Missions", Astronautics & Aeronautics, Vol. 8, No. 9, September 1970.

NASA/OSSA, "Launch Vehicle Estimating Factors", January 1971.

NASA/OSTI, "Planetary Flight Handbook, Space Flight Handbooks Volume 3," NASA SP-35, August 1963.

Rogers, A. E. E., and Ingalls, R. P., "Radar Mapping of Venus with Interferometric Resolution of the Range-Doppler Ambiguity", Radio Science, Vol. 5, No. 2 pp. 425-433 February 1970.

Thornbury, W. D., Principles of Geomorphology, John Wiley and Sons, Inc., 1961.

Uphoff, C., "The Long-Term Motion of Artificial Planetary Satellites", McDonnell Douglas Astronautics Comp., Western Div. MDC G1228, 1970.

Valcik, L., A Plan for Extensive Airborne Measurement of Radar Ground Clutter, IIT Research Institute, May 1971.